Spring 5-9-2020

A Raman Spectroscopic and Quantum Chemical Investigation of Serotonin, It's Intramolecular Interactions, and the Solvent Effects of Methanol, Ethanol, and Water

Mallory Loe

Raman Spectroscopic and Quantum Chemical Investigation of
Serotonin, its Intramolecular Interactions, and the Solvent
Effects of Methanol, Ethanol, and Water

by
Mallory Loe

A thesis submitted to the faculty of the University of Mississippi in partial fulfillment of
the requirements of the Sally McDonnell Barksdale Honors College.

Oxford
May 2020

Approved by

_____

Advisor: Dr. Nathan Hammer

_____

Reader: Dr. Randy Wadkins

_____

Reader: Dr. Jason Ritchie

i

ii

ACKNOWLEDGEMENTS

ABSTRACT

MALLORY MARGARET LOE: Raman Spectroscopic and Quantum
Chemical Investigation of Serotonin, its Intramolecular Interactions,
and the Solvent Effects of Methanol, Ethanol, and Water

(Under the direction of Dr. Nathan Hammer)

Serotonin, or 5-hydroxytryptamine, is a neurotransmitter and metabolite vital to the normal function of the cardiovascular, gastrointestinal, and nervous systems. Although it might be colloquially known as the 'happiness drug,' malfunctions in serotoninergic pathways can result in mental health disorders, heart disease, irritable bowel syndrome, and even collateral death. Without a current method to directly measure, or even detect, serotonin in the human body, these diseases, along with many others, pose a threat of developing without proper warning. Raman spectroscopy presents a unique method to vibrationally characterize molecules based upon the inelastic scattering of light. Serotonin's unique, amphipathic structure presents 69 vibrational modes that are observable under vibrational spectroscopy. Using B3LYP method and 6-311++G** basis set, the optimized structures of serotonin and various intramolecular structures were determined, and the results were Raman simulated. These spectra were compared to experiment collected for the crystalline solid, using a Horiba LabRAM spectrometer, 633nm excitation source, and over the 5-4000cm^{-1} range. The comparison lead to greater peak matchup than ever previously published of the Raman spectrum of serotonin. Because of its amphipathic nature, it is also interesting to consider interactions amongst serotonin with various solvents. Using the same level of theory, Raman systems were modeled for serotonin and solvents water, methanol, and ethanol. Theoretical results were studied to predict red and blue peak shifts that would be observed in experiment. Experimental data was collected with a custom Raman setup that vaporizes the solvent and assists its constant flow through the system by vacuum. The same spectrometer was used with a 532nm excitation source and collected over the 200-4000cm^{-1} range. The comparison of theory with experiment, although cut short due to the COVID-19 outbreak, lead to the successful observation of the solvent effects that methanol has on serotonin, as visible under Raman spectroscopy.

TABLE OF CONTENTS

LIST OF FIGURES, TABLES, AND EQUATIONS

LIST OF ABBREVIATIONS

5-HT	Serotonin		**FASD**	Fetal Alcohol Spectrum Disorders
α	Alpha		**GI**	Gastrointestinal
β	Beta		**gr**	Grating
Δ	Change in		**h**	Planck's Constant $(6.6.26*10^{-3}\frac{J}{s})$
λ	Wavelength (m)		**HF**	Hartree-Fock
ν	Frequency (incident)		**IR**	Infrared
ν_1	Frequency (shift in)		**Laser**	Light amplification by the stimulated emission of radiation
c	Speed of light in a vacuum $(\sim 3.00*10^8\frac{m}{s})$		**m**	Meters
CCD	Charge-Coupled Device		**nm**	Nanometers
cm	Centimeters		**NT**	Neurotransmitter
cm^{-1}	Wavenumbers		**Ser**	Serotonin
CNS	Central Nervous System		**SERS**	Surface enhanced Raman spectroscopy
CVS	Cardiovascular System		**TCS**	Temperature control stage
DFT	Density Functional Theory		**Trp / W**	Tryptophan
DI	Deionized		**UV-Vis**	Ultraviolet-visible
E	Energy		**X—H ...Y**	Hydrogen bond
EM	Electromagnetic		**YAG**	Yttrium Aluminum Garnet
ENS	Enteric Nervous System			

Chapter 1: Introduction

1.1 Bonding
1.1.1 Overview

Chemical bonds are present in molecules all around us and are characterized by a lasting attraction between atoms. Atoms are the most basic unit of matter and are made up of tiny, subatomic particles of varying charge. There are three major types of subatomic particles based upon their charge, and they are found in two separate regions of the atom, namely the nucleus and electron cloud. The nuclear portion contains protons and neutrons, which creates a positively-charged inner-sphere, whereas the electron cloud contains orbiting electrons, which results in a negatively-charged outer-sphere as shown in **Figure 1.1.1.1**. The positive nuclear portion of an atom is attracted to the negative electron cloud of another atom, which opens the door for bonding to occur. This attraction is considered electrostatic due to the difference in charge, with the favored interaction leading to a reduction in potential energy of the particles and, subsequently, bond formation [1]. Based upon the type of interaction occurring between the valence electrons of two atoms, the intramolecular bond can be classified as ionic, covalent, or metallic. Intramolecular bonding only occurs amongst atoms of differing partial charge but within the same molecule as shown in **Figure 1.1.1.2**. The other type of bonding results from intermolecular forces occurring between atoms of different molecules as demonstrated by the two hydrochlorides in **Figure 1.1.1.2**. These intermolecular forces are substantially weaker than intramolecular forces, but they are extremely useful in determining the physical properties of a compound such as its melting and boiling points. There are several

important types of intermolecular forces including: ion-dipole, hydrogen bonding, dipole-dipole, ion-induced dipole, dipole-induced dipole, and London dispersion forces (LDF) [2].
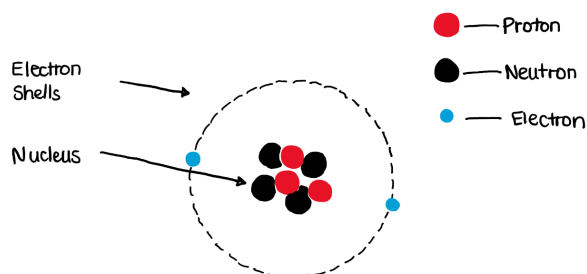
Figure 1.1.1.1: *Atomic Structure Labeled, adapted from reference [1]*
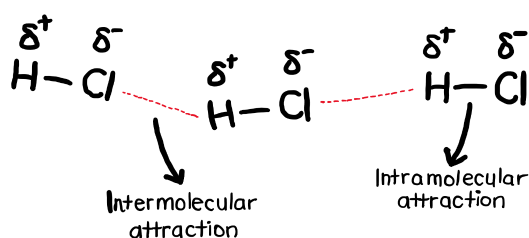
Figure 1.1.1.2: *Intramolecular and Intermolecular bonding, adapted from:*
https://www.khanacademy.org/test-prep/mcat/chemical-processes/covalent-bonds/

1.1.2 Hydrogen Bonding

Among the many types of intermolecular interactions, hydrogen bonding is arguably the most important to note. It is known that intermolecular forces are not as strong as ionic and covalent bonds, but hydrogen bonding is the strongest intermolecular factor and they are especially powerful when combined together in sequence. Notation is important when describing a hydrogen bond, with a common example being X—H ...Y. In this depiction, X and Y are both electronegative elements and the H would be a singular hydrogen atom. The hydrogen donor is always denoted by X, whereas the hydrogen accept is consistently Y as shown by the Hydrogen and Oxygen atoms in **Figure 1.1.2.1**, respectively. It should also be noted that the Y element standardly hold one or more lone pairs, which are causing the interaction. Fluorine, oxygen, and nitrogen are the three most common elements that form hydrogen bonds and can be easily remembered by the acronym

FON. Other elements are known to exhibit hydrogen bonding like carbon; however, the strength of the hydrogen bond with Carbon is much weaker than the ones listed above [3]. In any hydrogen bond, the hydrogen will attach to the most electronegative element and acquire a significant positive charge. The element being bound by a hydrogen will acquire a significant negative charge and requires at least one active lone pair. In order for the hydrogen bond to form, this active lone pair must initiate a charge transfer from the proton acceptor to the proton donor element. This charge transfer functions to weaken the X—H bond attraction and, subsequently, causes an increase in X—H bond length. This bond elongation is shown in experimental data by causing a decrease in the vibrational frequency. The observed variation of a bond frequency placement also possesses important notation. A shift to lower frequency of a spectrum is associated with a lower energy bond and is often denoted as a 'red shift'. When the vibrational frequency increases causing the energy to increase, a resulting 'blue shift' is denoted in turn [4,5].
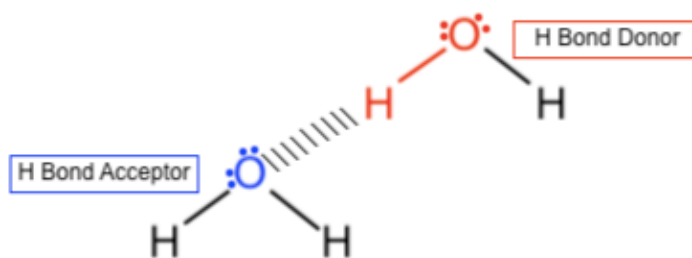
Figure 1.1.2.1: *Hydrogen Bonding General Structure, adapted from:*
https://www.studyorgo.com/blog/how-do-you-to-tell-when-a-hydrogen-bond-will-occur

1.2 Neurotransmitters
1.2.1 Overview

While cells of the nervous system function through electrical signals, chemical messengers, such as neurotransmitters, are critical at the junctions linking two neurons to enable the transfer of information across the gaps. Neurotransmitters make up a class of

endogenous chemicals that are released in order to spread signals quickly between brain cells. These messengers serve various purposes in the human body and their levels are heavily regulated through release, reuptake, generation, and metabolism. Each neuron typically produces only one type of neurotransmitter, which can be further classified into several groups including amino acids, monoamines, peptides, and purines [6]. Although the structure of neurotransmitters greatly varies, they are commonly very small and extremely important to greatly studied pathways such as acetylcholine in the parasympathetic nervous system and GABA in inhibition of neuronal activity.

1.2.2 Physiological Role

Neurotransmitters are generated in the cytosol of an axon terminal and generally function to communicate information throughout the body and brain. These chemical messengers are stored in synaptic vesicles, which are uniformly-sized organelles bound to the terminal. Upon arrival of an action potential at the axon terminus, voltage-gated calcium channels are opened and cytosolic calcium levels rise enough for ions to bind adjacent synaptic vesicles on the pre-synaptic membrane. Upon membrane fusion with calcium, neurotransmitters are released from the synaptic vesicles through exocytosis and the messengers travel across the extracellular cleft as shown in Figure **1.2.2.1**. The ability of a neurotransmitter to induce a response depends upon its binding to specific receptors in the postsynaptic membrane. When bound, the ion permeability of the postsynaptic membrane changes, initiates a cascade of chemical reactions, and serves to further transmit the chemical signal [7]. There are two major functions of a neurotransmitter which either promotes the generation or inhibition of an action potential within the post-synaptic

4

membrane. When neurotransmitters bind to an excitatory receptor, Na+ channels open in order to depolarize the plasma membrane and generate an action potential in the neighboring neuron. When neurotransmitters bind to an inhibitory receptor, Cl- channels open and function to hyperpolarize the post-synaptic membrane and prevent any action potential from occurring [8]. Interestingly, the same neurotransmitter is capable of binding to an excitatory or inhibitory receptor and promote a corresponding response in post-synaptic cells. For example, the neurotransmitter acetylcholine is known to be capable of binding to a receptor, depolarizing the membrane, and promoting signal transduction, while it can also bind, hyperpolarize the receptor, and effectively prevent the same signal cascade from initiating.
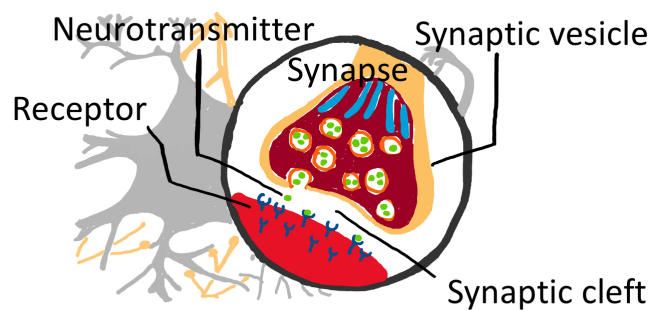
Figure 1.2.2.1: *Neurotransmitter Release and Structure of the Synaptic Cleft, adapted from reference [8]*

1.2.3 Neurotransmitter Metabolism
1.2.3.1 Overview

It is important to consider the synthesis, packaging, and re-uptake processes of neurotransmitters in order to understand how they are regulated in the human body. It has previously been noted that most neurons only generate one type of neurotransmitter, and most are synthesized by utilizing metabolites common to the cell and enzymes specific to the particular neuron. They are loaded into synaptic vesicles using transporter proteins and stored until stimulation, which further leads to vesicle-membrane fusion and exocytosis of

the neurotransmitters. After acting within the cleft, the free neurotransmitters must either be taken back up by the transporters that are reloading vesicles or destructed by transmitter-specific enzymes [9]. This process is highlighted in **Figure 1.2.3.1.1**, which depicts each step in the life of a generic neurotransmitter.
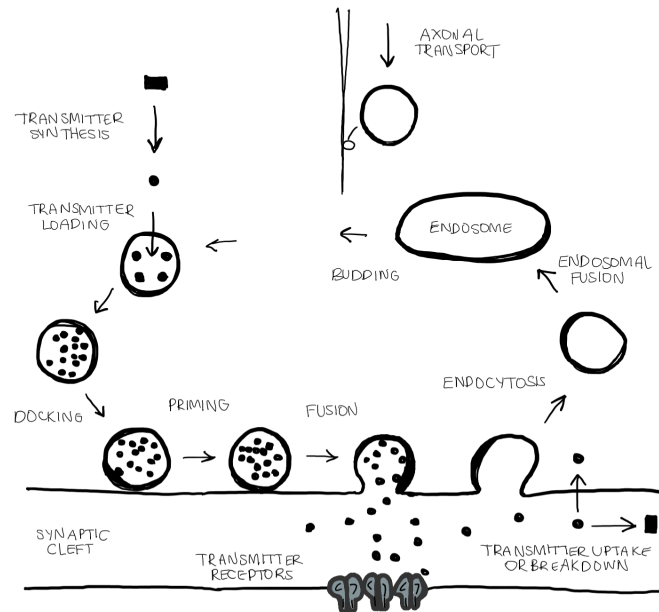
Figure 1.2.3.1.1: *Life Cycle of a Neurotransmitter, adapted from reference [9]*

1.2.3.2 Synthesis

In terms of synthesis, there are two types of neurotransmitters (NT) including small-molecule and neuropeptides. Small-molecule NT are created using byproducts of nearby chemical reactions and precursors imported by selective transporters on the membrane terminal. The enzymes necessary to catalyze the synthesis of small-molecule NT are typically generated in the cell body and transported to the terminal for their use. Where small-molecule NT are generated completely in the axon terminal, the synthesis of a neuropeptide NT is more complex due to its larger size and requires access to the genome in order for transcription, translation, and peptide bond formation to occur. Following a

similar path to other secretory proteins, a neuropeptide precursor undergoes post-translational processing resulting in a wide spectrum of NT products. Although the synthesis processes differ, both small-molecule and neuropeptide NT are stored in synaptic vesicles and undergo the same process for fusion and release [10].

1.2.3.3 Reuptake and Degradation

After a neurotransmitter is released from a synaptic vesicle, carries out its function by binding to receptors on the neighboring membrane, and returns to the cleft, it must be removed rapidly to enable the postsynaptic cell to engage in another cycle of signal transmission. In order to be removed from the cleft, the neurotransmitter must first diffuse into a nerve terminal or nearby glial cell. In most cases, the neurotransmitter will be picked up by a transport protein and repackaged into a synaptic vesicle in order to regenerate the cycle at the pre-synaptic terminal; however, in certain cases, the molecule will be marked for degradation by transmitter-specific enzymes [11]. The particular enzymes and transporters used for each neurotransmitter differs, but the general process remains the same. Referring back to **Figure 1.2.3.1.1**, this process is depicted and useful to compartmentalize the simultaneous processes.

1.2.4 Systems Interaction with Alcohol

It has long been accepted that alcohol groups interact with fetal neurotransmitter systems throughout development upon exposure, most notably ethanol with biogenic amines such as serotonin and dopamine. These interactions can lead to fetal alcohol spectrum disorders (FASD) as demonstrated in multiple animal models, which showed that even low levels of exposure during any singular trimester of pregnancy can result in FASD

7

[12]. These disorders can result in multiple compounding impairments and an increased susceptibility to neuropsychiatric and neurological disorders such as substance abuse, depression, and epilepsy. For this reason, it is recommended for expecting mothers to abstain from any alcohol use in order to prevent FASD from developing in their child [13].

Into adult life, a particular neurotransmitter's actions, Serotonin, has been linked to alcohol's effects on the brain. It has been suggested that alcohol regulates the neurotransmitter's levels in the synapses of brain cells and even modifies the activities of serotonin-specific receptor proteins in the post-synaptic membrane [14]. It should be noted that the relationship between serotonin levels and alcohol exposure has not been studied directly due to the lack of ability to measure serotonin concentrations in the human brain. Instead, only metabolites of the neurotransmitter have been monitored through blood, urine, and the cerebrospinal fluid. Through these studies, it has been shown that individuals consuming copious amounts of alcohol show differences in serotonin levels, typically lower metabolite concentrations measured, compared with non-alcoholics [15]. This relationship has pointed to extensive alcohol consumption leading to altered Serotonergic signal transmission in the brain, which is also indicative of ongoing psychological problems or mental illness.

1.3 Serotonin
1.3.1 Structure and Properties

Serotonin, or 5-Hydroxytryptamine, has a molecular formula of $C_{10}H_{12}N_2O$ and is a primary amino compound derived from tryptamine. Serotonin has a molecular weight of 176.21 g/mol, exists in nature as a solid with a melting point at 167.5 °C, and it is soluble in water at 25.5 mg/mL [16]. **Figure 1.3.1.1** is a microscopic picture of crystalline Serotonin

using the CCD camera on the Raman spectrometer. **Figure 1.3.1.2** demonstrates the molecular geometry of Serotonin depicted using Molekel software.
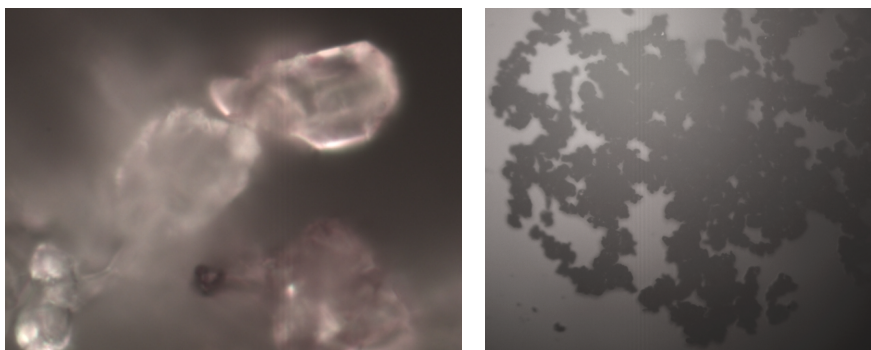
Figure 1.3.1.1: *Crystalline solid serotonin pictured using the CCD camera*
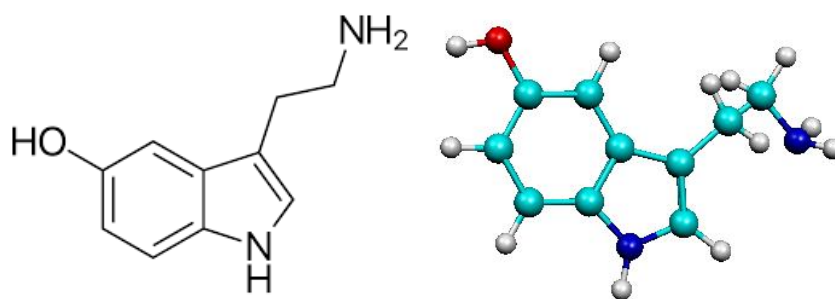
Figure 1.3.1.2: *Molekel Demonstration of 5-Hydroxytryptamine (Serotonin)*

1.3.2 Physiological Role

Serotonin (5-HT) is a biochemical messenger functioning as a human metabolite and has a local transmission role in multiple organ systems. Serotonin not only acts as a neurotransmitter in brain cells but also functions as a signaling molecule in both intestinal cells and blood platelets. **Figure 1.3.2.1** shows the series of metabolic reactions resulting in the synthesis of serotonin from the amino acid L-tryptophan, which involves a hydroxylation and decarboxylation step. This process would occur in the central nervous system (CNS), specifically within the Raphe nuclei located in the brainstem, although the Serotonin end-product is transported and stored in several other locations throughout the

body. The precursor amino acid tryptophan is obtained through the diet and its absorption

is partially responsible for regulation of serotonin levels [17].
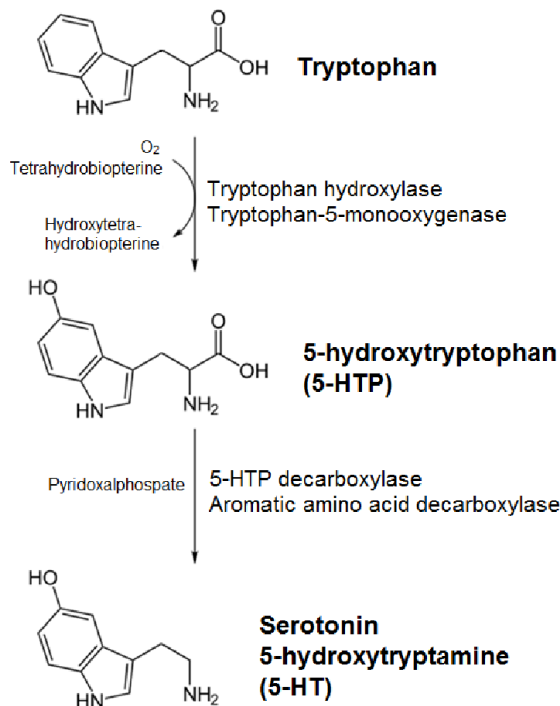
Figure 1.3.2.1: *Series of reactions deriving Serotonin from L-tryptophan, adapted from:*
https://www.researchgate.net/publication/273640973_Serotonin_serotonin_receptors

1.3.2.1 Serotonin and the Central Nervous System

Serotonin is a monoamine neurotransmitter arguably best known for its role in

synapses of the central nervous system (CNS). The molecule's action is thought to promote

feelings of well-being and happiness when correctly modulated [18]. There are several

hypotheses relating the dysregulation of this neurotransmitter and abnormal function of the

CNS, including an increase of psychological problems and even development of various

mental illnesses. Selective Serotonin Reuptake Inhibitors (SSRIs) have long been used as

a treatment of psychological disorders and promote the normal functioning of pathways

associated with Serotonin's physiological role such as mood, sleep, and appetite. SSRIs

target the reabsorption time of serotonin within the synapse, with an increase of time

available for the neurotransmitter's action in the synapse typically corresponding to a more normally-regulated CNS.

1.3.2.2 Serotonin and the Gastrointestinal System

Although commonly referred to in the CNS as the happiness drug, Serotonin is actually primarily found in the enteric nervous system (ENS) and is specifically located in enterochromaffin cells of the gastrointestinal tract (GI tract). In fact, approximately 90% of the human body's total serotonin is located in the GI tract, where it functions to regulate intestinal movements through its action on intrinsic nerves of the intestinal lumen [19]. When stimulated, enterochromaffin cells release serotonin stores and promote the normal peristaltic reflex; however, alterations in this intestinal pathway have been linked to irregular speed of gastrointestinal motility and diseases such as irritable bowel syndrome.

1.3.2.3 Serotonin and the Cardiovascular System

Serotonin also has an agonistic role in platelet formation during agitation and vasoconstriction of the cardiovascular system (CVS). When released from storage in platelets and into the blood stream, serotonin binds to specific-target receptors, which are structurally similar to those on the post-synaptic membrane, and initiates a signal cascade. The resulting events following the binding of the neurotransmitter include the amplified release of other vasoconstrictors, such as angiotensin and norepinephrine [20]. As always, it is important to consider the dysregulation of this signal cascade to emphasize the importance of this physiological pathway. Abnormalities in the cardiovascular Serotonergic system have been linked to multiple diseases including hypertension and

peripheral vascular disease and helps confirm the importance of Serotonin to the overall normal function of the heart.

1.4 Alcohol Groups of Interest

An alcohol is any organic molecule that contains an -OH group on a terminal end. It has already been noted that any hydrogen atom attached directly to an oxygen or nitrogen is capable of hydrogen bonding (FON acronym), and these interactions occur to strengthen the compactness of a molecule. The presence of hydrogen bonding in a molecule also corresponds to a greater amount of energy needed to break its chemical bonds. Alcohol groups are special because they are capable of both proton donation and acceptation, which leads to extensive interactions as solvents in solution [21]. Serotonin, due to its own alcohol group and two nucleophilic amines, is capable of hydrogen bonding with other solvents with alcoholic structures. Three notable alcohols should be emphasized when considering serotonin's hydrophilic interactions including ethanol, methanol and water.

1.4.1 Ethanol

The interactions between serotonin and ethanol in the human body has puzzled scientists for a long time and is possibly linked to the central nervous system's normal functions. For this reason, it is important to consider the molecule both theoretically and experimentally interacting with serotonin in order to observe the shifts in vibrational frequencies resulting from solvation.

1.4.1.1 Structure and Properties

Ethanol is a clear, colorless liquid with a molecular mass of 46.07 g/mol, and structure as shown in **Figure 1.4.1.1.1**. Its molecular formula is C_2H_6O and it is often used

as a topical disinfectant, solvent, and a primary ingredient in alcoholic beverages. It is thought to have a depressive effect on the central nervous system and is, therefore, considered to be a drug due to its psychoactive properties. Ethanol is capable of binding to several neurotransmitter post-synaptic receptors including serotonin and can also stimulate its release [22].
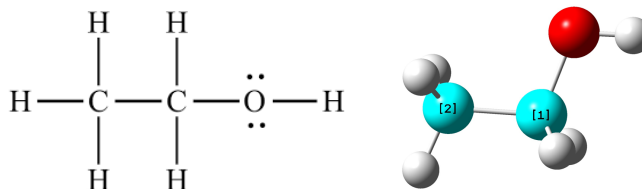
Figure 1.4.1.1.1: *Molecular Structure of Ethanol depicted by Gaussview*

1.4.2 Methanol

Unlike ethanol, methanol is toxic to humans and even considered a poison. For this reason, it is not typical to consider the interactions amongst serotonin and methanol in a normal-functioning physiology. It is, nonetheless, still interesting to study the solvent effects of the molecule with serotonin in order to understand further the molecule's tendencies to form hydrogen bonds with various alcohol groups.

1.4.2.1 Structure and Properties

Methanol is a colorless, fairly volatile liquid with a molecular mass of 32.04 g/mol. Its molecular formula is CH_3OH and its structure is shown in **Figure 1.4.2.1.1**. Methanol is considered the primary alcohol, with the simplest aliphatic formula, and is often used as a solvent, a fuel, and is a common metabolite in many species including humans. Methanol is an intermediate in many synthesis pathways and is also capable of interacting with Serotonin as an alcohol through hydrogen bonding [23].
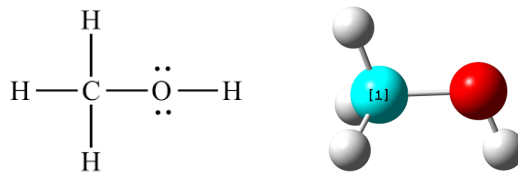
Figure 1.4.2.1.1: *Molecular Structure of Methanol depicted by Gaussview*

1.4.3 Water

Water is essential to many physiological pathways, including the transformation of the amino acid tryptophan into serotonin. In order for the amino acid to transmit through the blood-brain barrier, water is necessary. For this reason, it is important to consider the molecule's interactions with serotonin and understand where the hydrogen bonding might occur and the results seen in a vibrational spectrum.

1.4.3.1 Structure and Properties

Water is a colorless liquid with a molecular mass of 18.01 g/mol. Its molecular formula is HOH (or more commonly, H_2O) and its structure is shown in **Figure 1.3.2.1.1**. Because alcohols are considered organic derivative of water, synthesized by replacing a hydrogen atom with an alkyl group, and demonstrates both acidic and basic properties. It is often used as a solvent and is essential for survival of any living organisms. Water is also capable of interacting with Serotonin with its alcohol group through hydrogen bonding [23].

Figure 1.4.3.1.1: *Molecular Structure of Water depicted by Gaussview*

1.5 Spectroscopy

There has been debate over the nature of matter and light for centuries, which ultimately lead to our current classification of a relationship named spectroscopy.

14

Spectroscopy is described as the study of the interactions between light and matter. When Christiaan Huygens and Isaac Newton disagreed over the nature of light being wave or particle-like, Einstein ultimately solved the debate using a particle-wave duality description with the need for both theories in order to fully explain light. In the meantime, Newton had discovered the crude spectra of sunlight, but the significance of using a narrow slit, instead of a pinhole or round aperture, was later independently discovered by W. H. Wollaston and Joseph Fraunhofer. This discovery allowed lines to be visible on spectra, which represented different wavelengths of light involved. Then, G. R. Kirchhoff and R. Bunsen demonstrated the importance of spectroscopy in the field of chemical analysis while discovering new alkali metals in the late 1800s. Finally, M Planck's research during the 20th century concerning quantum theory lead to a simpler explanation of light as a stream of particles, which are known today as photons. The following equation, developed by Planck, describes the energy of a photon (E), where h is Planck's constant, and v is the frequency in hertz [24].

$$E = hv = \frac{hc}{\lambda} \qquad (1.5.1)$$

1.5.1 Electromagnetic Radiation

In order to contextualize the light being studied, the electromagnetic spectrum needs to be described as involving all waves which couple electric and magnetic fields. Although these particle-waves exist as photons, electromagnetic radiation consists of oscillating electric and magnetic fields that propagate through space along a linear path and with a constant velocity. Typically, photons are designated by their wavelengths or energies, respectively, and divided into groups based upon these values as shown in **Figure**

15

1.5.1.1. This figure also depicts the equation in **1.5.1**, which demonstrates wavelength and energy as having an inverse relationship. It should also be noted that the visible range is expanded in order to highlight their wavelengths as being distinguishable [25].
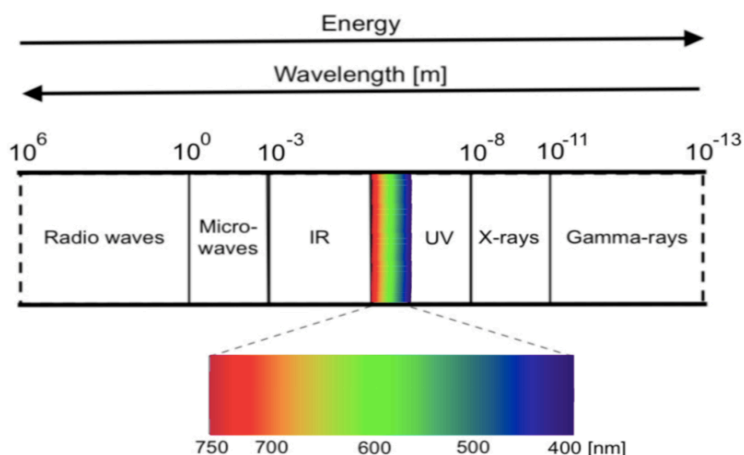
Figure 1.5.1.1: *The Electromagnetic Spectrum, adapted from reference [26]*

1.5.2 Transitions

A transition occurs when there is a change in the energy of a molecule, which might take place after any change in motion or electron energy within the molecule. Most molecules exist in their ground state at room temperature, which is also the lowest energy state. When light, an excitation source, hits a sample of matter, the light can take several paths. Light can be absorbed, transmitted, reflected, or scattered by the sample. An excitation source can excite a molecule at ground state to an elevated state, which is described as a transition that would show up on a spectrum. There are multiple possibilities of transitions between energy levels in molecules, and the energy of these transitions is increasing in the order: translational < rotational < vibrational < electronic. These transitions are observed in different regions of the electromagnetic spectrum based upon the energy difference of the ground and excited state for the particular movement. Allowed

transitions are shown in **Figure 1.5.2.1** and are separated by their respective energy transition type. Transitions in rotational states, for example, lead to spectra in the microwave region. Transitions involving vibrational states produce spectra in the infrared region. This makes sense due to the wavelength of microwaves being relatively long, and lower in energy, than the infrared region. Transitions can also occur in electronic states of molecules which can produce spectra in the visible and ultraviolet regions. There is also the possibility of a rovibrational transition, involving both a rotational and vibrational transition, which describes one that is not purely electronic in nature [26].
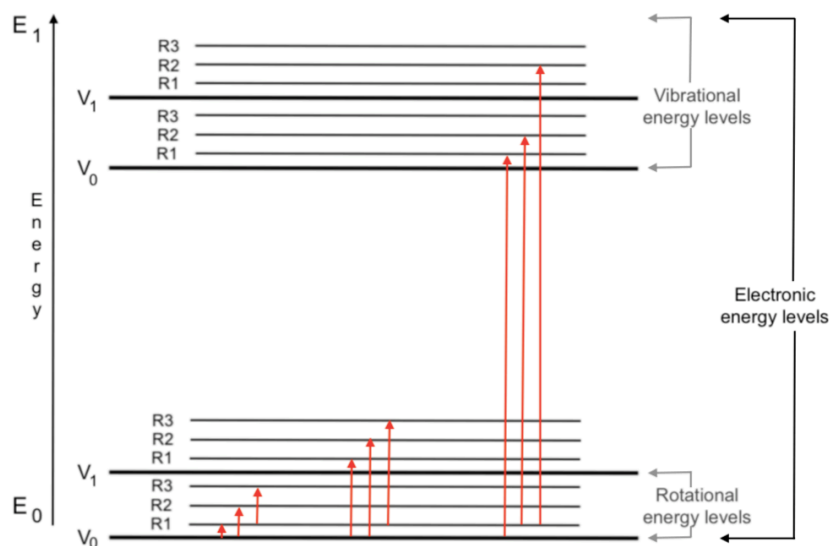
Figure 1.5.2.1: *Energy level diagram describing allowed transitions, adapted from [26]*

1.5.3 The Harmonic Oscillator

Vibrational transitions are modeled by the harmonic oscillator and can be explained with both classical physics and quantum theory. If a particular spring is attached to a mass, m, being held stationary, it can be considered under a classical physics approach and Hooke's law applied. In this case, the force on the spring is proportional to the displacement, x, of the mass as shown in **Equation 1.5.3.1**, where k is the force constant

and is a measure of the rigidity of the spring. The force can also be modeled, however, using **Equation 1.5.3.2**, which describes V as the harmonic potential and assumes that the spring is stretched out infinitely far and then back in the other direction.

$$F = -kx \qquad (1.5.3.1)$$

$$F = -\frac{dV}{dx} \rightarrow V = \frac{1}{2}kx^2 \qquad (1.5.3.2)$$

For the quantum mechanical harmonic oscillator model, consider instead two masses held together by a Hooke's law spring. In this case, the displacement of the spring from its initial location, R, and returning to its equilibrium location, Re, can be shown as x = R − Re. This value can be inserted for the Hamiltonian, which specifies both the kinetic and potential energy of a system in the Schrodinger Equation as shown in **Equation 1.5.3.3**. The eigenvalues of this equation represent the energy levels of the harmonic oscillator and appear as straight horizontal lines in the harmonic oscillator model to an infinitely high quantum number. Because there are only two masses in this system, there is only one, nondegenerate quantum number present and a simplified expression results for the harmonic oscillator as seen in **Equation 1.5.3.4** [27].

$$\widehat{H} = \frac{-\hbar}{2\mu}\frac{d^2}{dx^2} + \frac{1}{2}kx^2 \qquad (1.5.3.3)$$

$$\nu_0 = \frac{1}{2\pi}\sqrt{\frac{k}{\mu}} \qquad (1.5.3.4)$$

1.5.4 Vibrational Spectroscopy

Vibrational spectroscopy is a class of methods by which only the interaction of radiation with molecular vibrations is studied. It is used to study a vast array of sample types, in either bulk or microscopic amounts, under a wide range of temperatures, and in any state of matter. The steps can be carried out to form a simple identification test up to

an in-depth, full spectrum, qualitative, and quantitative analysis of the sample. Two different approaches are used for the interpretation of vibrational spectroscopy data. The first approach is the use of group theory along with mathematical calculations of the forms and frequencies of the molecular vibrations. The second approach is the use of empirical characteristic frequencies for chemical functional groups. Both should result in the elucidation of the molecular structure of the sample being studied. The two major vibrational methods, Infrared and Raman spectroscopy, differ in the manner in which photon energy is transferred to the molecule during a vibrational transition. Certain molecules are active under Infrared spectroscopy, others Raman, and some are active under both methods [28].

When molecules exhibit transitions amongst vibrational modes, a corresponding stretch or bend occurs that can be identified based upon its frequency. Dependent upon whether the transition correlates to a stretching or bending mode, there exist several vibrational motions that could occur. Where stretching modes typically change the bond length while maintaining bond angles, bending changes the bond angle while maintaining bond length. Concerning stretching modes, there exist two forms being symmetric and antisymmetric, whereas bending can result in scissoring, wagging, rocking, or twisting. These modes and their motions are demonstrated in **Figure 1.5.3.1** with the blue circles representing atoms of a general molecule. Bending modes are typically lower in frequency and appear in the fingerprint region of an Infrared spectrum, although they are rarely seen in Raman spectroscopy due to consistent bond length and, therefore, consistent polarizability [29]. **Table 1.5.4** provides the proper symbols commonly used for naming vibrational modes and the motions that they represent.
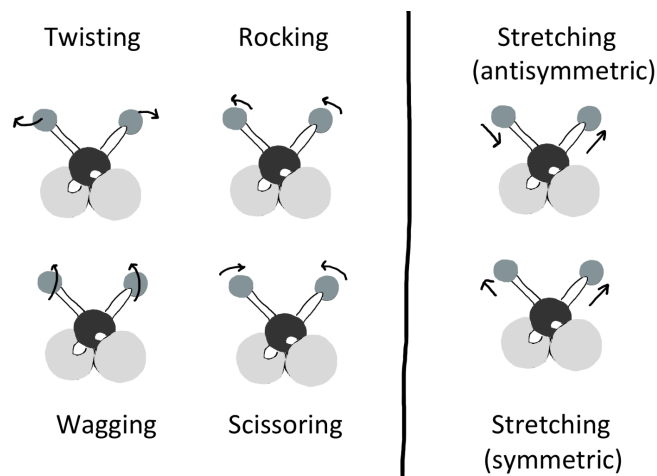
Figure 1.5.4.1: *Vibrational modes as differentiated by motion, adapted from:*
https://www.semanticscholar.org/paper/IR-spectroscopy-for-vibrational-modes

Mode	Symbol	Planar ring deform.	α (R)
Stretching	ν	Twisting	τ
Planar deformation	β	Wagging	ω
Non-planar deform.	γ	Scissoring	σ
Non-planar ring deformation	φ (R)	Rocking	ρ
Butterfly Mode	b.f.	Angle Bending	α

Table 1.5.4: *Vibrational Mode Symbols*

1.6 Raman Spectroscopy
1.6.1 Introduction

In 1923, the Raman effect was first predicted by Smekal and observed by Raman himself 5 years later. The first experiments Raman ran focused on sunbeams and relied on the visual observation of color changes due to scattering light after placing filters in the line of sight. In later years, Raman used a mercury lamp and spectrograph to record spectra of several liquids and observed an inherently weak effect from the incident radiation making the process altogether very difficult in comparison to the developed infrared spectrometers. However, a major improvement occurred when a new, amplifying factor was used as an additional source to the lamp, followed by the introduction of

commercial CW visible lasers. These improvements have led to Raman spectroscopy becoming a standard analytic technique with applications in multiple research fields. This method provides an interesting choice for many scientists due to its sensitivity to small structural changes, its non-invasive or destructive sampling capability, the minimal sample preparation required, and the resulting high spatial resolution especially in Raman micro-spectroscopy [30]. Although these spectrometers can have various set ups, each machine must have the same key components including the monochromatic light source and a detector, which is typically a charge coupled device (CCD) acting to convert scattering photons into an electrical signal on a computer. This set up is shown in **Figure 1.6.3.1** and highlights these key components along with a spectrograph grating, acting to disperse light into a frequency spectrum.
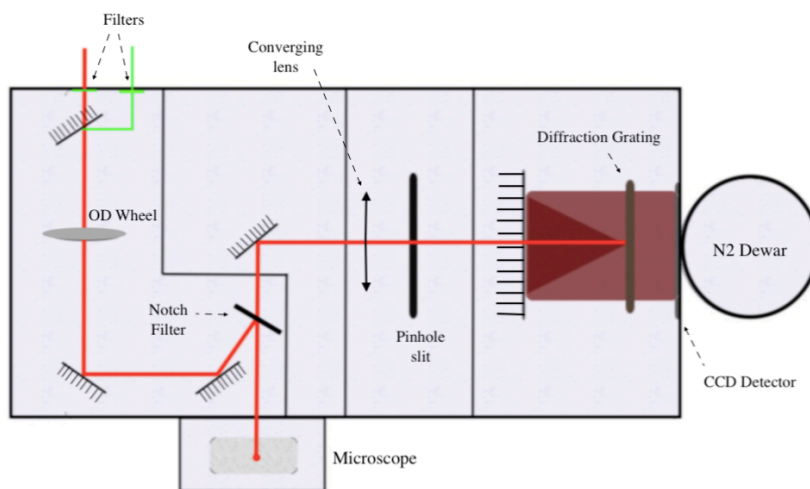
Figure 1.6.1.1: *Schematic Diagram of a LabRAM Raman spectrometer*

1.6.2 Background and Theory

The Raman effect states that there exists a change in wavelength that is exhibited by scattered radiation in a medium. The classical approach to the Raman effect regards the scattering molecules simply as a collection of atoms undergoing harmonic vibrations while

not considering any quantization of vibrational energy. This process can be seen in **Figure 1.6.2.1**, which demonstrates both elastic and inelastic scattering. Elastic scattering, or Rayleigh, is not observed in Raman spectroscopy because there is no change in wavelength and these photons are scattered without any change in energy. This happens for most photons of monochromatic light interacting with a molecule, which explains the low magnitude observations of inelastic scattering in spectra. It should also be noted that in order for a Raman shift to occur, a change of polarizability must occur in the molecule after interacting with the incoming light. A small number of photons are inelastically scattered upon interaction, undergoing a change in energy, and either lose energy to the molecule resulting in an excited, vibrational state known as a stokes shift or gain energy from the molecule resulting in a lower vibrational state known as an anti-stokes shift. As previously stated, however, most molecules are in the ground state at room temperature and this points to a greater probability of a stokes shift occurring [31].
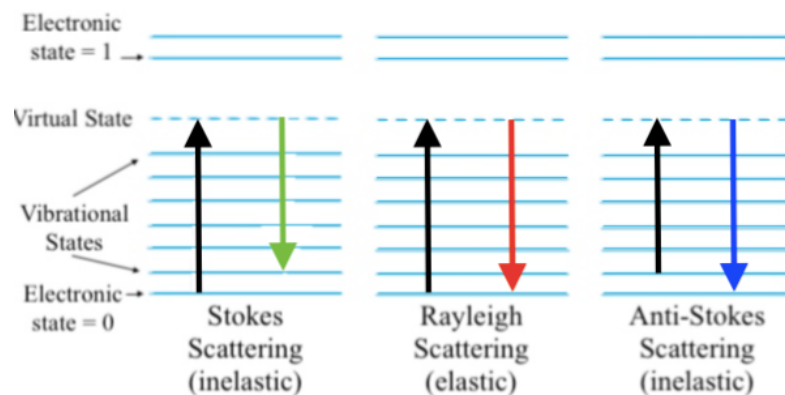
Figure 1.6.2.1: *Diagram of Rayleigh and Raman (stokes/anti-stokes) processes, adapted from: https://www.researchgate.net/publication/275274523_Evaluating _Biomass*

1.6.3 Raman Light Source

The standard excitation component of a Raman spectrometer, typically a laser, stands for Light Amplification by Stimulated Emission of Radiation. When commercial

CW visible lasers were introduced to Raman spectrometers, these monochromatic, narrow beam lasers transformed the capability of the method to record spectra more comparable to the less expensive and well-developed infrared spectrometers. CW lasers operate at extremely high intensities and led to easily recordable spectra from small sample volumes, colored samples, and from multiple states of matter including gas, solid, and liquid samples. The wavelength of the incident laser is chosen is chosen such that it will optimize interaction with the sample particles in order to resonate, and the apparatus will therefore record the greatest intensity of the scattered light. Today, Raman spectra can be recorded in as little as nanoseconds due to the optical multichannel analyzers that detect the spread of wavelengths scattering from a sample [32]. **Table 1.6.3.1** is a table showing the several most common lasers that can be used in a Raman setup, along with their corresponding wavelengths. Deciding which laser to use is important in order to minimize fluorescence scattering from a sample, which tends to drown out the Raman signal.

Laser Type	Wavelength	Krypton	416 nm
Argon	454.6 nm	Nitrogen	337.1 nm
HeNe	632.8 nm	CO_2	10.6 um

Table 1.6.3.1: *Table demonstrating common lasers used in Raman Spectrometers*

1.7 Computational Chemistry

Most experimental findings in physical chemistry are confirmed through the use of theoretical methods. These methods, most commonly computations, serve to determine and optimize the molecular structure of the compound being studied. From the various conformations possible, computations approximate the lowest-energy formation of these and further calculate vibrational stretching modes that would be expected when studying

the molecule under experimental methods, such as spectroscopy. Upon 360° rotation of a molecule in a Newman projection presentation, several distinguishable structures result with different amounts of energy bound based upon the angle of torsion. For example, a full 360° rotation of ethane leads to three identical "staggered" structures, which are energy minima, and three identical "eclipsed" structures which are energy maxima as shown in **Figure 1.7.1**. This energy plot is important for computations to optimize the structure of a molecule, which is always the lowest, or minimized, energy conformation.
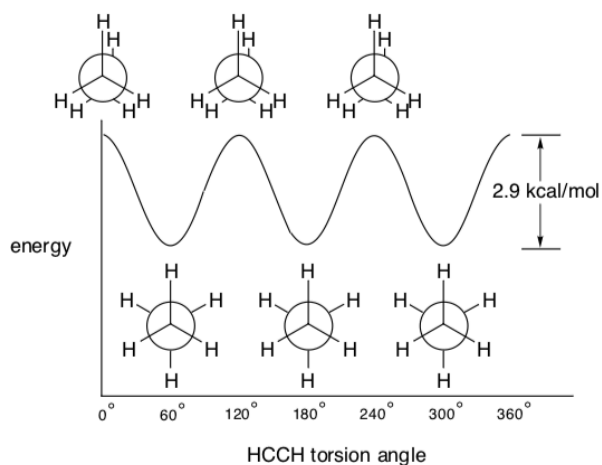
Figure 1.7.1: *ΔE of ethane as a function of the $<_{torsion}$ about the C-C bond, adapted from reference [43]*

Other than identifying the lowest-energy conformers of a particular molecule, these approximation methods can even calculate vibrational frequencies and generate theoretical spectra for comparison to the experimental results. Using theory provides chemists with an opportunity to study chemicals that are either highly reactive, not found in nature, or simply difficult to obtain through the use of a broad range of programs and techniques. One of the most important aspects of computational chemistry is the application of quantum software in order to approximate the Schrodinger equation and provide the lowest-energy molecular structure that would be favorable if the molecule being studied were to exist in nature or

during a chemical reaction. The Schrodinger equation, in its simplest form, is shown in **Equation 1.7.1**, where E is the total energy of the system, and $\hat{H}$ is described as the Hamiltonian, which specifies both the kinetic and potential energy for the particles. Because it is impossible to solve the Schrodinger equation for multi-atom systems, it is necessary to make approximations so that the answer can be estimated [26].

$$\hat{H}\psi = E\psi \qquad\qquad (1.7.1)$$

1.7.1 Hartree-Fock Molecular Orbital Theory

Today, there exists software and computer programs that are capable of approximating the Schrodinger equation in a manner that is satisfactory in comparison with experimental results. In other words, although the exact answer cannot be predicted due to an insolvable equation needed for the particular answer, approximation programs today are developed enough to be used in real-life implications comfortably. The Hartree-Fock (HF) Molecular Orbital Theory is one of the oldest approximation programs to date, which applies the Born-Oppenheimer equation in order to solve the Schrodinger wavefunction, Ψ. This approximation is shown in **Equation 1.7.1.**1 and assumes that from the perspective of orbiting electrons, the nucleus is stationary and thus removes the nuclear-nuclear Coulombic energy term. The Hartree-Fock approximation itself deals with electrons moving in complete independence of one another and, therefore, each electron, N, feels the same average field of energy, N-1, and is confined to a spin orbital. This assumption poses a setback for the Hartree-Fock method with the idea that electrons are always paired, but this is not always the case. Approximations are okay in theoretical chemistry, but it should be kept in mind that each one applied in order to make a theory work is also pushing the method farther away from the actual, experimental result [33].

25

$$\hat{H}^{el}\psi^{el} = E^{el}\psi^{el} \qquad (1.7.1.1)$$

1.7.2 Density Functional Theory

In an effort to expand upon the capability of the Hartree-Fock Method, the Density Functional Theory (DFT) was introduced based in order to consider a multi- electron system and propose an exact solution, but it operates only under the idea of an electron gas with a uniform density. In DFT, the energy of a system is calculated as the sum of six different components. They are expressed in **Equation 1.7.2.1,** where E_{NN} corresponds to the nuclear nuclear-repulsion, E_T corresponds to the kinetic energy of electrons, E_V corresponds to the nuclear-electron attraction, E_{coul} corresponds to the electron-electron Coulomb repulsion energies, E_{exch} corresponds to the non-classical electron-electron exchange energies, and E_{corr} corresponds to the correlated movement of electrons with different spins. In summary, DFT functions to compensate for the more natural characteristics of the electrons in a system, including spin and interactions between electrons, which are absent from the HF method [26].

$$E_{DFT} = E_{NN} + E_T + E_V + E_{coul} + E_{exch} + E_{corr} \qquad (1.7.2.1)$$

1.7.3 Optimizations and Frequencies

In order to calculate the optimized structure of a particular molecule, it is first necessary to find the lowest energy point on its potential energy surface (the bottom of the energy well on a coordinate diagram). It should be noted that although the optimization calculation does not always provide the lowest-energy structure, it does ensure at least a local-minima and is lower in energy than the original structure. This is important due to the feasibility of using theory to represent the probability of a particular conformation to

exist in nature. The process of geometry optimization occurs in a series of steps including derivatives with respect to geometry coordinates, energy calculations and formation of a gradient, making a guess based upon these values, and then redirecting based upon the outcome. In order for a geometrical guess to be deemed correct, the energy gradient must approach zero. Once pinpointed, this optimized structure can be further analyzed for theoretical frequencies of the vibrations that would be produced during Raman spectroscopy and even simulate a spectrum to compare to experimental data. These values are found based upon the simulated vibrations in a molecule resulting in a change in polarizability and representing the particular motion as Raman active on the spectrum [26].

Chapter 2: Previous Research

Serotonin, or 5-hydroxytryptamine, has become a hot topic to study in biochemical research over the past decade. With a rising knowledge about its importance to multiple organ systems including the cardiovascular, gastrointestinal and central nervous systems, there still does not exist any form of technology to directly monitor levels of Serotonin *in vivo*. Instead, some of its metabolites are monitored in urine, blood, and cerebrospinal fluid, however, these values are not necessarily a trustworthy predictor. Serotonin's physiological functions include its involvement in numerous metabolic pathways, which results in uncertainty when measuring metabolites from only one pathway. Thankfully, there have been rapid developments in the field of biomedical optics over the past decade, with technology now capable of tracking certain molecules based upon their distinctive fingerprints visible through vibrational spectroscopy. Because of this, it has recently become feasible to detect important biological compounds in the human body systems based upon their characteristic frequencies appearing in spectra.

Before 2005, Serotonin had not been experimentally studied under any form of vibrational spectroscopy according to published literature. During this year, S. Bayari and colleagues successfully recorded the first vibrational spectrum of Serotonin using the potassium bromide pellet technique under Fourier Transform Infrared Spectroscopy (FTIR), with their best published figure provided here in **Figure 2.1**. Their group compared the fundamental modes observed in the experimental spectrum with several levels of theory, although the B3LYP/6-31G(d) method gave the best correlation [34]. Although our

group aims to obtain the Raman spectrum of the molecule, IR is a complementary technique useful for accuracy comparisons. Their determination of B3LYP as the optimal method also helped guide our own decision for which theoretical approach to use.
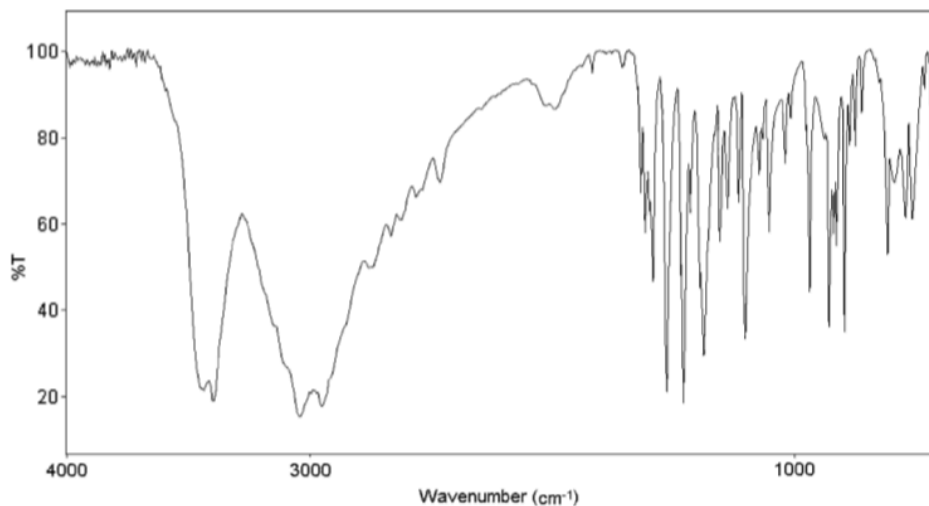
Figure 2.1: *FTIR Spectrum of 5-HT in KBr [34]*

The same Bayari group also did a short experimental study concerning the solvent effects of 5-HT in H_2O, D_2O, and Ethanol solutions. For these measurements, the group used FTIR and their results showed that some of the spectral bands in solid state changed their intensities and positions in the transition to liquid state. They also determined that most of the bands observed in solid state spectra disappeared or overlaid in solution, resulting in far less distinguishable spectra. With this data almost devoid of a fingerprint region entirely, it was determined that the solvent effects of H_2O, D_2O, and Ethanol are heavy [34]. Our own group saw this result as a challenge to experimentally measure the solvent effects of alcoholic groups on Serotonin, especially in the fingerprint region, using our high-resolution ultralow frequency capabilities.

In 2009, the Zwier group thoroughly studied the solvent effects of water clusters on Serotonin conformers through utilization of a jet-cooled supersonic expansion to form

singular and double water clusters around the monomer. Initially, the Zwier group determined the three lowest-energy conformers of a serotonin-water cluster using DFT M05-2X/6-31+G* calculations. These results were labeled A, B, and C in order of increasing energy, as shown in **Figure 2.2**, and were used for the remainder of the simulated experiments [35]. Our group was able to utilize these structures for our own calculations to confirm and expand upon their knowledge of the noncovalent interactions occurring between alcoholic groups and serotonin.

| Gph(out)/*anti* | Gpy(out)/*anti* | Gpy(out)/*syn* |
| 0 | 4.83 | 5.31 |
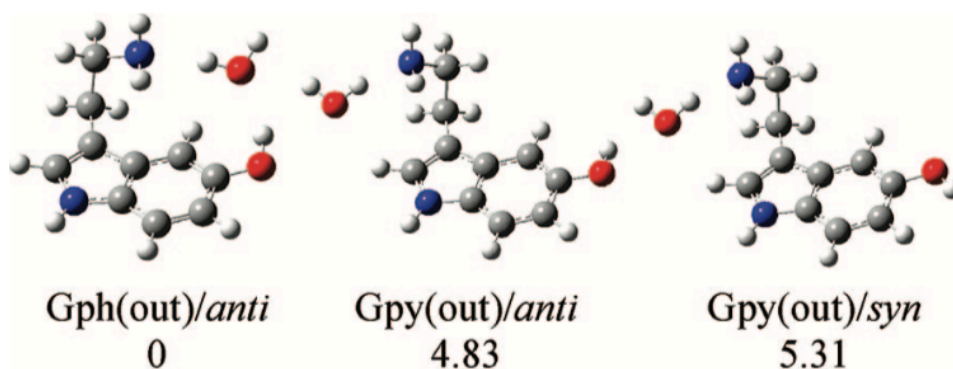
Figure 2.2: *LE conformers of a serotonin-water cluster (A, B, and C, respectively)* [35]

Next, the Zwier group used resonant ion-dip infrared (RIDIR) spectroscopy and a jet-cooled gas expansion device to experimentally record spectra of the A, B, and C clusters shown above. In addition, the lowest energy conformer of a serotonin-(water)$_2$ cluster was determined, IR simulated, and experimentally collected by altering the gas-phase ratios. The group used DFT B3LYP/6-31+G* method and basis set, which showed satisfactory matchup to their published experimental data and is provided here in **Figure 2.3** [35]. The peak shifts are noted in their works and utilized by our group for accuracy comparison. Our group also wished to expand upon the knowledge of these serotonin-water interactions by using higher level of theory, utilizing our greater resolution capabilities in the fingerprint region, and simulating spectra using structures with greater solvent:serotonin ratios.
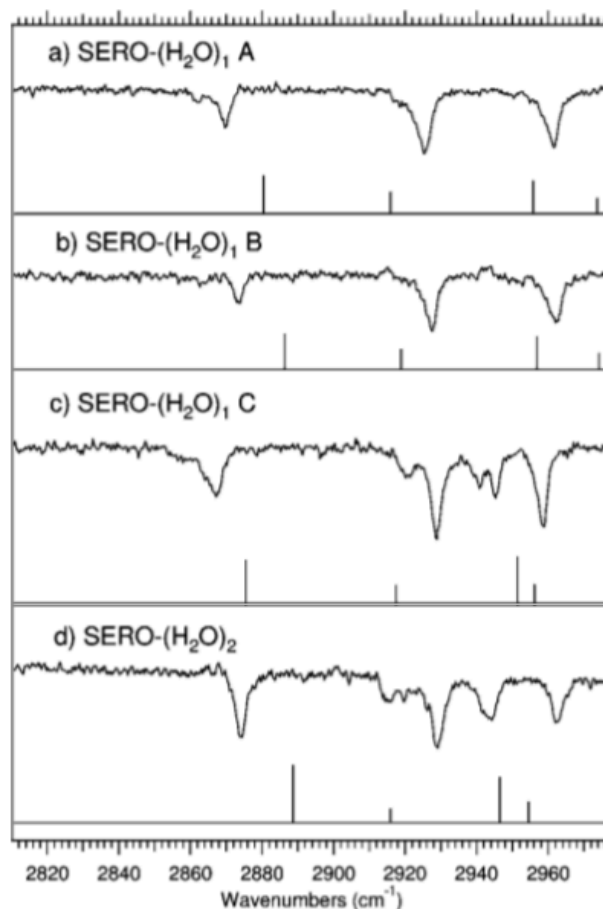
Figure 2.3: *RDIR spectra of A,B,C, n₂ Serotonin-water clusters compared with theory* [35]

Arguably most relevant to this thesis, A. Priya and colleagues published a study covering hydrogen-bonded complexes of serotonin with methanol and ethanol in 2014. Their research was restricted to DFT theory, but their findings were very beneficial to identify ten stable interacting conformers of serotonin with singular methanol and ethanol molecules. Their DFT findings noted that interactions amongst serotonin and ethanol are much stronger than with its counterpart methanol. The ethylamine side chain was also identified as the most reactive site in both methanol/ethanol complexes with serotonin, and all levels of theory were carried out with B3LYP method 6-311++G(d,p) basis set. Next, natural bond orbital (NBO) analysis confirmed for the group that a C–H…O hydrogen

31

bond indeed formed between the serotonin–alcohol complexes in the presence of both methanol and ethanol. Finally, the decomposition analysis revealed that strong interactions between serotonin and ethanol/methanol are, in fact, due to the attractive contributions from the electrostatic component present in the groups [36]. This group's research provided knowledge of the predicted interacting points within a serotonin-methanol and serotonin-ethanol cluster, identified the lowest energy conformers, and left room for optimization improvement through a higher level of theory.

For the first time in 2016, the Raman spectra of Serotonin was published by J. Omkant and R. Yadav. Their group determined the lowest energy conformer of the neurotransmitter using optimization calculations with the B3LYP method and 6-311++G** basis set, which is an extremely high level of theory. Using this optimized configuration and the same level of theory, the vibrational spectrum of Serotonin was simulated and compared to experimental spectra collected using a HORIBA HR 800 Raman spectrometer in the 50-4000 cm^{-1} range and a solid powder sample from Sigma Aldrich. Although their procedure noted that the purchased sample was a white crystalline solid, their calculations were run for the Serotonin monomer and not a crystallized molecule. Due to this, the shapes of the resulting peaks were different and crystallization noted as a source for the discrepancies seen in the spectra. Their experimental spectrum is provided below in **Figure 2.4**, which was used for accuracy comparison to our own observed and simulated peaks. Their graph also appears as a low-resolution spectrum that our group aimed to improve upon with a more precise instrument and greater parameters used.
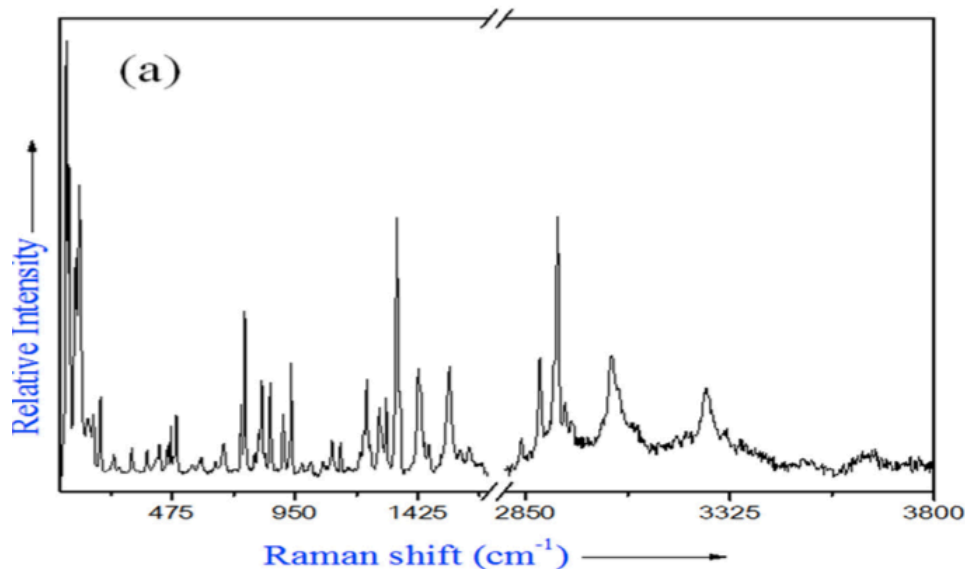
Figure 2.4: *Experimental Raman Spectrum of Serotonin* [37]

The most successful and thorough research of serotonin to date was carried out by F. Manciu and colleagues in 2017 and studied the computational and experimental analysis of the neurotransmitter on silver nanocolloids, utilizing Surface-Enhanced Raman Spectroscopy (SERS). SERS typically provides a dramatic enhancement of the optical signal scattering analyte being investigated; however, it requires a lengthy preparation which would not be favored in a biomedical application where concentrations are constantly changing if the normal Raman spectrum could also be captured. The group used a 532 nm Nd:YAG laser restricted to 100μW and a 20x objective on an alpha300 R WITec spectrometer. Although the SERS study was successful, it also published one of the first normal Raman spectra of the monomer Serotonin as seen in **Figure 2.4,** which our group is more interested in and will be attempting to compare to in the initial part of our own study. When compared to their level of theory at B3LYP 6-311++G(d,p), the discrepancies between the experimental and computed vibrational frequencies was 9 ± 2 cm^{-1}, on average [38]. The correlation is the highest to be published so far, but there still exists a higher level

33

of theory that might prove an even better match. The figure the group published is provided

below in **Figure 2.4**, although this is not the correct spectrum for Serotonin. Our own group

suspects that there was a mix up in the data, because although their peaks match-up between

theory and experiment, the frequencies are altogether different from previously published

works and even the source their group cited to confirm their experimental spectrum.
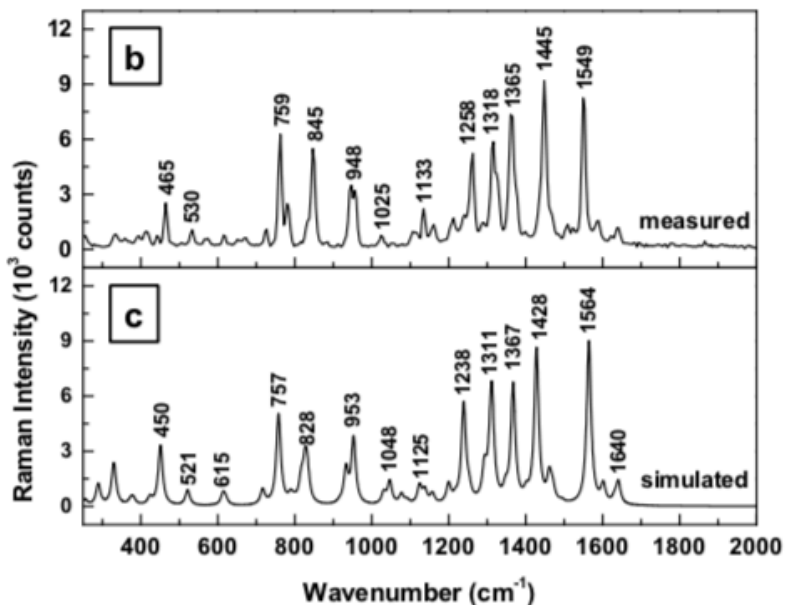
Figure 2.5: *Experimentally measured calculated Raman vibrations of Serotonin* [38]

The Manciu group, as previously stated, also published theoretical and experimental SERS

spectra of serotonin for three conformers, which proved to have excellent correlation with

theory and is provided below in **Figure 2.5**. The vibrational frequencies in these figures,

although interacting with silver, match up to our own group's simulated and experimental

data without Ag present. The peaks observed are different, however, for the group's own

SERS and normal Raman collections, which is wholly unexpected for these methods and

further points to confirm our own suspicious of a mistaken figure being published. This

realization left room for our own group to publish high resolution Raman data of

monomeric serotonin that is accurate and can be confirmed by various methods. The Manciu group's work, ultimately, was aimed to improve upon a previous study of Serotonin using SERS analysis [39], which they successfully completed with little room for improvement.
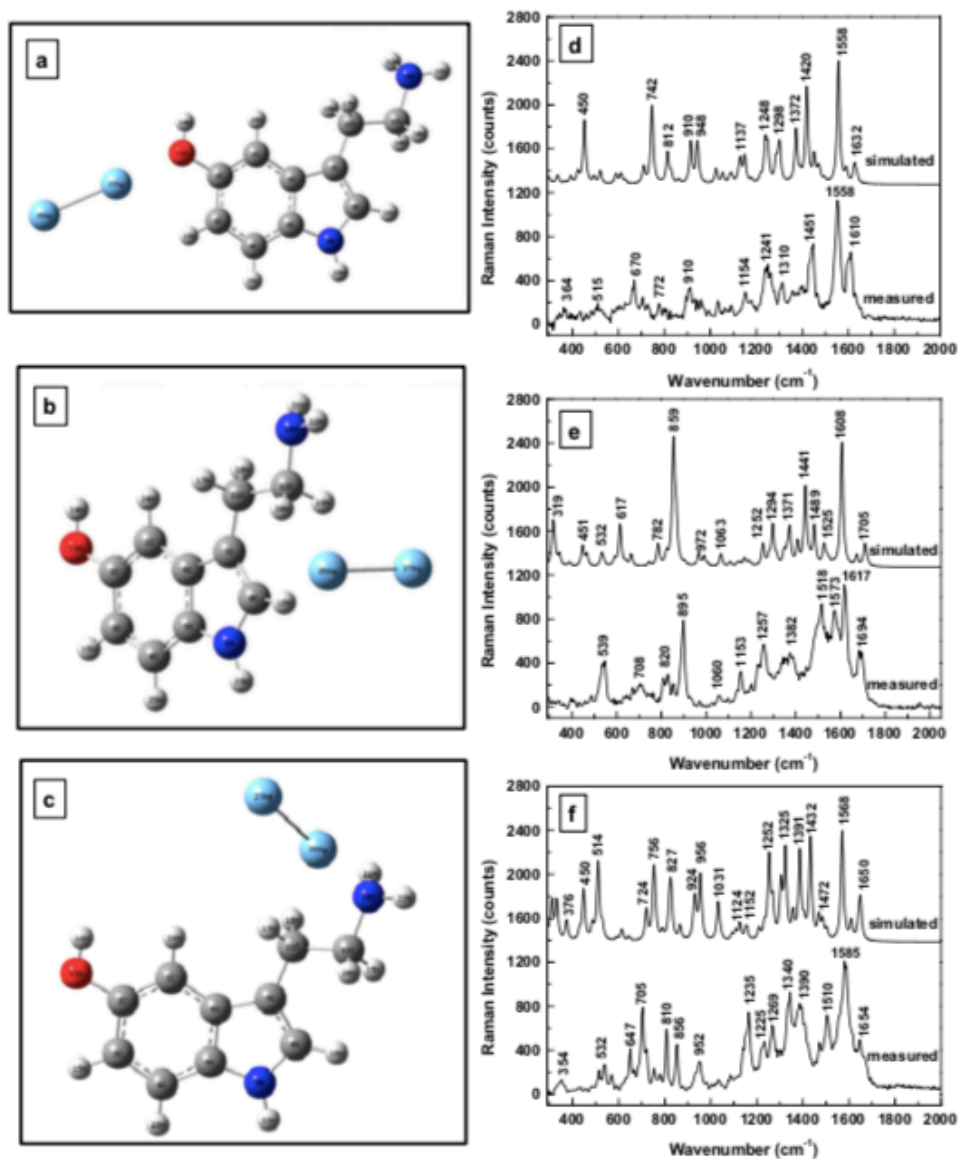
Figure 2.6: *SERS theoretical / experimental analysis for three serotonin conformers* [38]

Several other groups have since published similar SERS analyses of Serotonin with comparable results [40, 41]. The following have covered SERS as a potential biosensing

detection technique for Serotonin and other neurotransmitters and concluded that the molecules could only be detected reliably with amplification of signal by SERS-active substrates [40]. This group used SERS due to the amplification of signal detection for a molecule that is already fairly Raman active, which our own group aimed to confirm. The other referenced study, also by the Manciu group, studied Serotonin's interactions with another neurotransmitter Dopamine in various concentrated solutions under SERS analysis and is not as relevant to our own interest in alcoholic interactions [41].

In an attempt to expand upon the knowledge of Serotonin's apparent crystalline structure in the solid state, M. Borah and colleagues carried out the vibrational analysis of both the Serotonin monomer and its dimer with the B3LYP method and 6-311++G* basis set in order to assign the vibrational modes of the structures. These simulated spectra were compared with experimental data of the purchased Serotonin solid from Sigma Aldrich and using a Horiba X-Ploral Micro-Raman system with an excitation source at 785 nm diode laser [42]. Although the group's attempt was thorough and followed an optimal protocol, their theory and experiment did not match up well as shown in their published spectra provided below in **Figure 2.7**. This data shows peaks that appear wholly different, both in size and location, for theory and experiment. The group hypothesized that the sample might not have been accurately detected, potentially due to the use of a relatively low-power laser, leading to such a lack of peak match-up. Our own group suspected that a higher laser power might solve their subdued signal problem and provide better peak matching. The study was still beneficial to reference, however, due to their optimized structure of the serotonin dimer and simulated spectra with high level of theory.
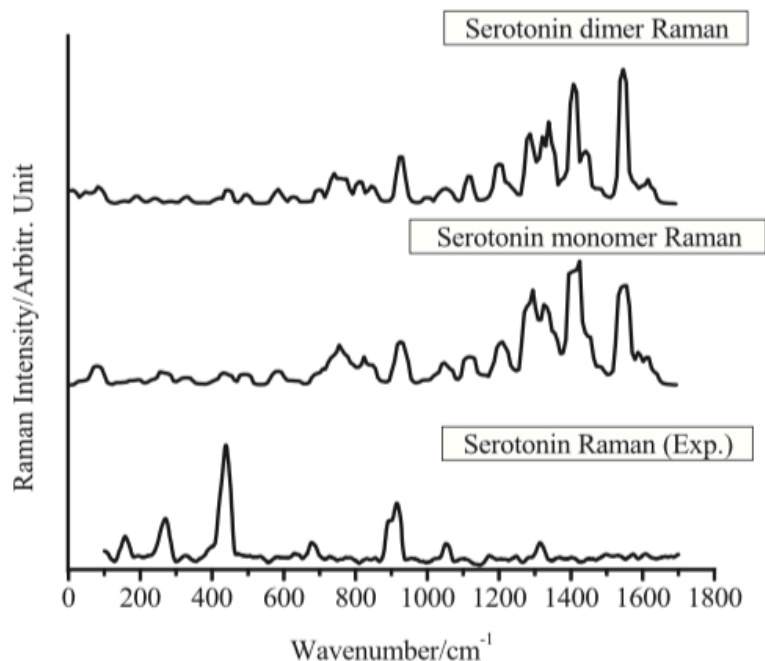
Figure 2.7 *Simulated and Experimental Raman Spectra of Serotonin* [42]

No one to date has successfully published a high-resolution experimental spectrum of the solid, crystalline Serotonin that matches up the theory. For this reason, our group has attempted to study the solid as compared to both monomer, dimer, and crystalline state in theory to determine the best correlation with experimental data. Additionally, no one has published an analysis of the neurotransmitter Serotonin following a theoretical versus experimental format concerning its interactions with water, methanol, and ethanol, which leads to our own group's angle in this thesis.

Chapter 3: Theoretical Methods

3.1 Methods and Basis Sets Background

B3LYP is a common method of the density functional theory, specifically a hybrid functional, and is attempting to recover electron correlation through approximation. The hybrid functional idea mixes exchange energies that are calculated with those from DFT methods in an exact manner to ensure the best possible calculation. B3 is referring to Becke's three-parameter exchange correlation functional, which unsurprisingly uses 3 parameters. LYP refers to the Lee Yang and Parr correlation functional that recovers dynamic electron correlation, where the combination of these is shown in **Equation 3.1.1**:

$$E_{XC} = 0.2E_X(HF) + 0.8E_X(LSDA) + 0.72DE_X(B88)$$

$$+0.1E_C(LYP) + 0.19E_C(VWN) \tag{3.1.1}$$

The three scaling factors seen in the equation are derived by fitting the correlation parameters to various sets of thermochemical data in literature [43].

The name of a particular basis set is a reflection of a specialized field of quantum chemistry, which uses a systematic abbreviation method. Basis sets for HF, DFT, and many other methods utilize gaussian functions, which are closely related to exponential functions. This project utilizes a split-valence basis set, which calls for an inner and outer function to compensate for a non-spherical environment. A split-valence basis set represents core atomic orbitals by one set of functions and valence atomic orbitals by two sets of functions, and this project works up to the 6-311++G(2df,2pd) level of theory. In ley terms, this basis set represents core atomic orbitals in terms of six Gaussians and

valence orbitals are split into three parts, with three and one and one Gaussian components, respectively. The parentheses contain general polarization functions, which represent a Taylor series expansion of the overall function in order to compensate for displacement of electron distributions away from the nuclear positions. For these expansions, the first term always refers to core atoms and the second term to hydrogen atoms in the molecule being investigated. In this case, (2*df*) implies that two sets of *d* and one set of *f* polarization functions are added to all non-hydrogen atoms, and (*2pd)* that two sets of *p* and one set of *d* polarization functions are added to hydrogen atoms. The + denotes a diffuse set to be included and, in this case, is compensating for both the core and non-hydrogen atoms [44].

3.2 Computation Series

Because B3LYP 6-311++G(2df,2pd) is an extremely high level of theory and the systems being studied are fairly large, the calculations are run in series based upon previous checkpoint files using the Gaussian 09 program. All geometry optimization calculations are run under the B3LYP method, beginning with 6-31G on a loose grid, followed by this basis set at default, then running the full 6-311++G(2df,2pd) expansion. Finally, the Raman frequencies of the optimized geometry can be predicted through the command "freq=raman" and based upon the optimized checkpoint file. Initially, this series of events was carried out for the monomer Serotonin, then the intermolecular interactions between the compound with water, methanol, and ethanol were investigated. These cluster-systems were studied by using the lowest energy conformer of Serotonin with the surrounding, small molecule being placed in four positions as shown in **Figure 3.1.1** and represented as position A, B, C, and D. Although these images depict the placement of water amongst

serotonin, the placement (A,B,C,D) of the alcohol group remained the same for the methanol and ethanol systems, only with added terminal methyl groups to consider. Once the optimized geometry was discovered for the system using the highest level of theory, the Raman spectrum was simulated and would be later correlated with experimental data.

Ser + 1wA   **Ser + 1wB**

Ser + 1wC   **Ser + 1wD**
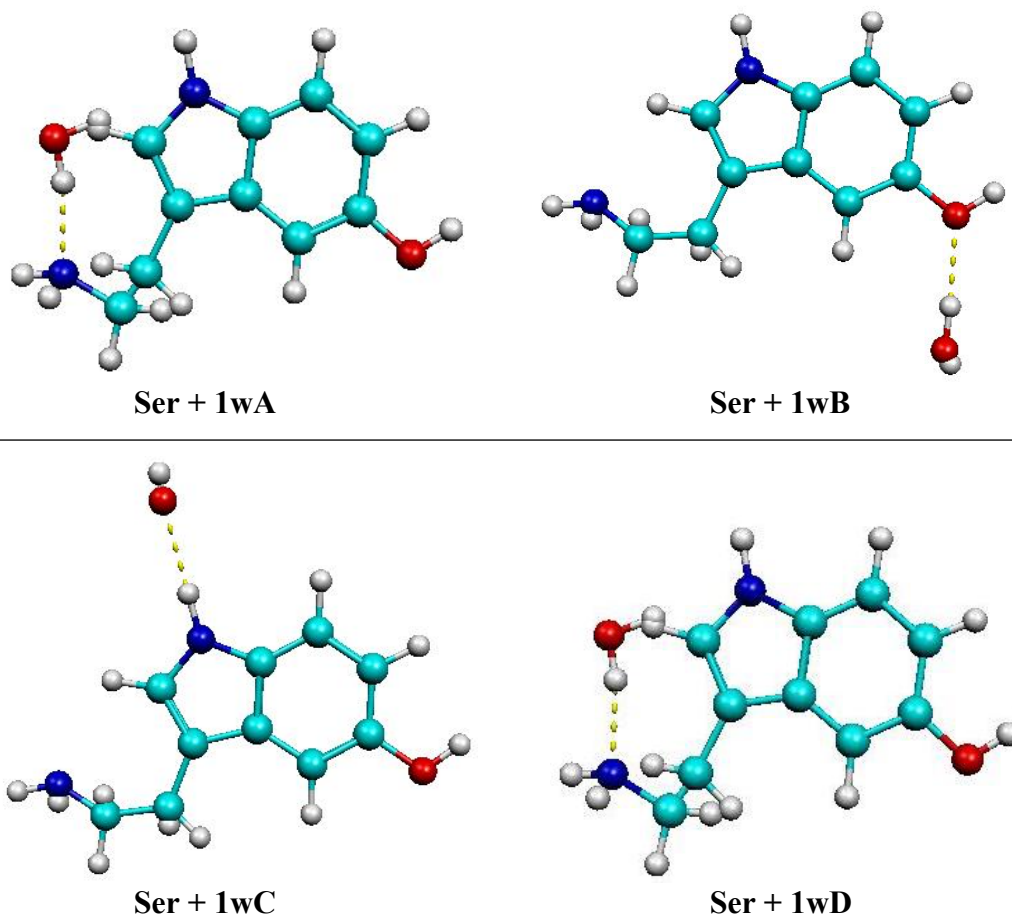
Figure 3.2.1: *Serotonin-water Clusters in Four Different Configurations*

3.3 Data Collection
3.3.1 Serotonin Monomer

The structure of the serotonin monomer was previously shown in **Figure 1.3.1.2** and accurately represents the molecular model being simulated in the following

calculations using the B3LYP method and 6-311++G** basis set. Both the geometric optimization and Raman frequencies were calculated and presented below.
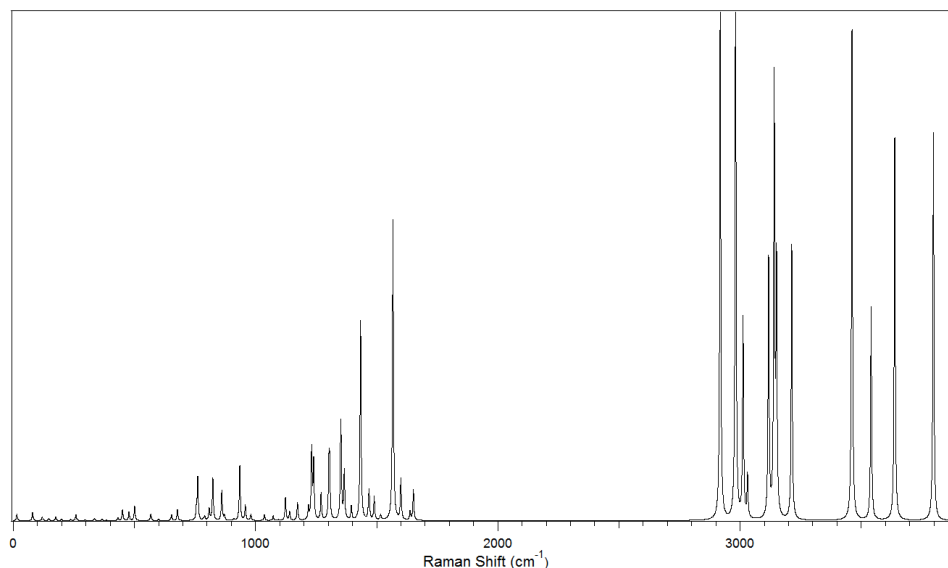
Figure 3.3.1.1: *Full Simulated Raman Spectrum of Serotonin*

The simulated Raman spectrum of the serotonin monomer resulted in peaks that are both clear and sharp, as expected, although the varying intensities make it difficult to analyze all at once. For this reason, the full spectrum was initially provided for proof of the success of the method, and the analysis will subsequently be carried out using subsections of the above spectrum. Because there are no apparent peaks present in the 1900-2800 wavenumber region, this section was left out of the ensuing analysis portions to enhance the resolution of peaks being studied. The 69 vibrational modes observed in the full spectrum were then viewed using the GaussView program for motion, and the assignable modes, along with their frequencies, are provided in **Table 3.3.1**. It should be noted that, according to the Born Oppenheimer approximation that describes the degrees of freedom for vibrational motions (3N-6), the monomer serotonin ought to have 69 vibrational modes and, due to having C_1 symmetry, all modes are expected to appear in spectral analysis.
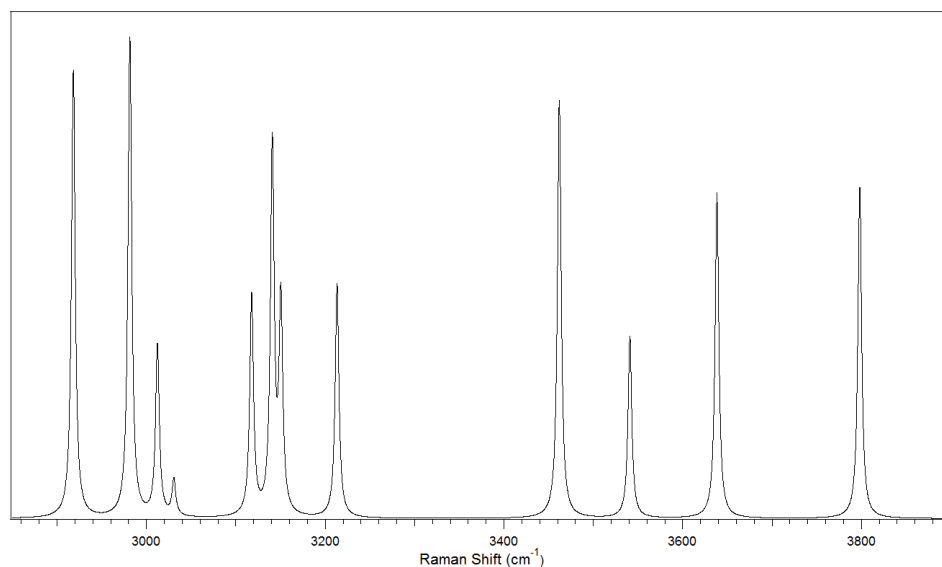
Figure 3.3.1.2: *Low Frequencies of Simulated Raman Spectrum of Serotonin*
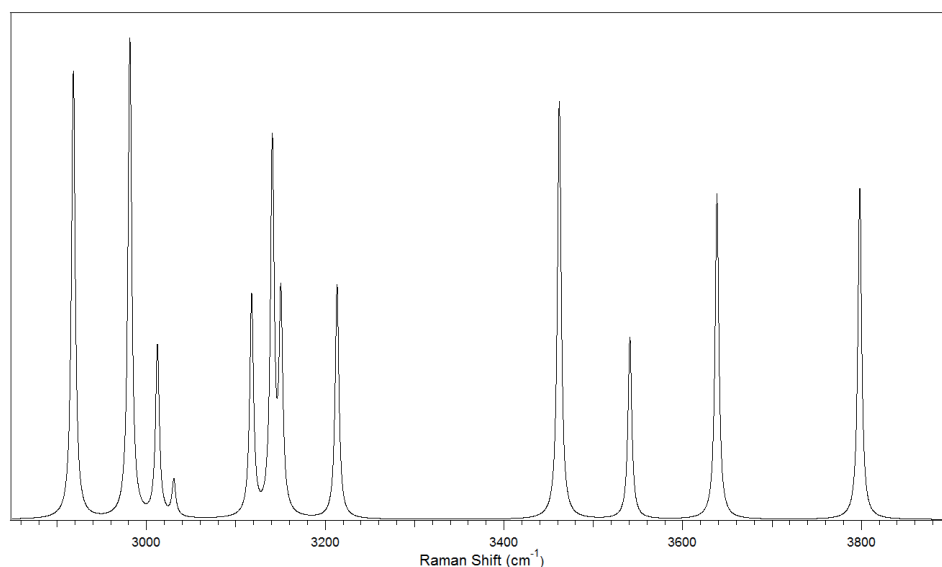
Figure 3.3.1.3: *High Frequencies of Simulated Raman Spectrum of Serotonin*

ν	cm⁻¹	Motion		cm⁻¹	Motion		cm⁻¹	Motion
1	14.54	τ (C-C)	**10**	335.25	b.f (R_1-R_2)	**20**	677.56	υ (C-C)
2	79.50	γ (C-C)	**11**	366.5	α (C-C-N)	**21**	755.56	ϕ (ring)
3	119.41	τ (C-C)	**12**	384.38	β (C-OH)	**22**	761.09	α (ring)
4	146.92	γ (C-OH)	**13**	431.70	ϕ (ring)	**23**	785.07	τ ($^{20}CH_2$)
5	174.70	α (C-C-C)	**14**	450.80	ϕ (ring)	**24**	790.20	γ (C-H)
6	199.87	β (C-C)	**15**	477.46	α (ring)	**25**	808.40	γ (C-H)
7	236.29	τ (NH_2)	**16**	500.56	α (ring)	**26**	823.51	ω (NH_2)
8	258.04	τ (O-H)	**17**	567.50	ϕ (ring)	**27**	860.54	γ (C-H)
9	295.70	τ (N-H)	**18**	600.00	α (ring)	**28**	871.58	ν (ring)
			19	653.01	ϕ (ring)	**29**	910.91	γ (C-H)

#	cm⁻¹	Mode	#	cm⁻¹	Mode	#	cm⁻¹	Mode
30	934.84	ν (ring)	44	1305.5	ν (C-OH)	58	2918.2	ν_s ($^{20}CH_2$)
31	957.65	ν (C-C)	45	1351.3	ω ($^{17}CH_2$)	59	2981.4	ν_s ($^{17}CH_2$)
32	980.76	α (ring)	46	1352.8	β (C-H)	60	3012.3	ν_{as} ($^{20}CH_2$)
33	1036.5	ν (C-NH$_2$)	47	1366.2	ν (ring)	61	3030.6	ν_{as} ($^{17}CH_2$)
34	1072.6	τ ($^{20}CH_2$)	48	1395.4	ω ($^{20}CH_2$)	62	3117.7	ν (C-H)
35	1094.3	β (C-H)	49	1433.4	β (N-H)	63	3140.8	ν (C-H)
36	1123.5	β (C-H)	50	1466.1	σ ($^{17}CH_2$)	64	3150.4	ν (C-H)
37	1140.3	ρ (NH$_2$)	51	1468.8	ν (ring)	65	3213.3	ν (C-H)
38	1172.9	α (COH)	52	1489.6	σ ($^{20}CH_2$)	66	3461.9	ν_s (NH$_2$)
39	1218.3	β (C-H)	53	1516.4	ν (ring)	67	3540.9	ν_{as} (NH$_2$)
40	1231.5	ν (ring)	54	1567.1	ν (ring)	68	3638.3	ν (N-H)
41	1239.6	ν (ring)	55	1600.0	ν (ring)	69	3798.1	ν (O-H)
42	1270.3	ρ ($^{17}CH_2$)	56	1637.7	σ (NH$_2$)			
43	1302.5	ρ ($^{20}CH_2$)	57	1651.4	ν (ring)			

Table 3.3.1: *Assigned Modes for the Simulated Raman Spectrum of Serotonin*

3.3.2 Serotonin Dimer and Trimer

In order to account for the serotonin powder being a crystal, it is important to consider the crystallization of 5-HT in this quantum chemical investigation. Because the pure crystal structure of serotonin has never been published, our group aimed to begin with structurally optimizing three different dimers to shed light on the favorable interactions amongst monomers themselves. **Figure 3.3.2.1** shows the three interacting sites that were used to create electrostatically interacting dimers of Serotonin, in which a Ser AA dimer would be two monomeric forms noncovalently interacting at the A sites for both molecules. The Hartree-Fock energies associated with each of the dimeric structures is provided below in **Table 3.3.2.1** and help indicate where the monomers most favorably interact with one another. These dimers were structurally optimized to indicate the energy associated with the conformation using the B3LYP method and 6-311++G** basis set. The structures were then simulated under Raman spectroscopy to predict peak transformation, most typically seen in shape and intensity, for the dimeric structures.
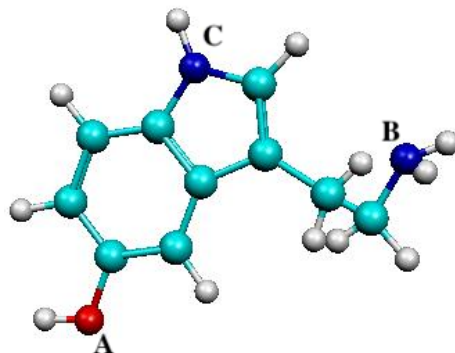
Figure 3.3.2.1: *Molekel depictions of Ser interacting sites A,B, and C*

Conformer	Energy (Hartrees)
Ser dimer A/A	-1146.3568491
Ser dimer A/B	-1146.3523372
Ser dimer A/C	-1146.3566923

Table 3.3.2.1: *HF Energies of the three serotonin dimers*
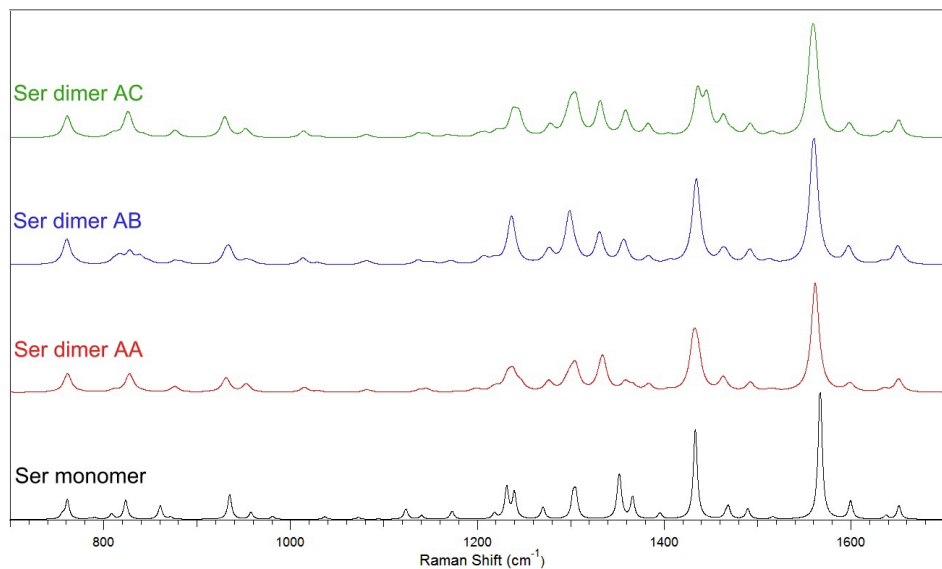
Figure 3.3.2.2: *Low Frequencies of Simulated Serotonin dimer Raman Spectra*

44
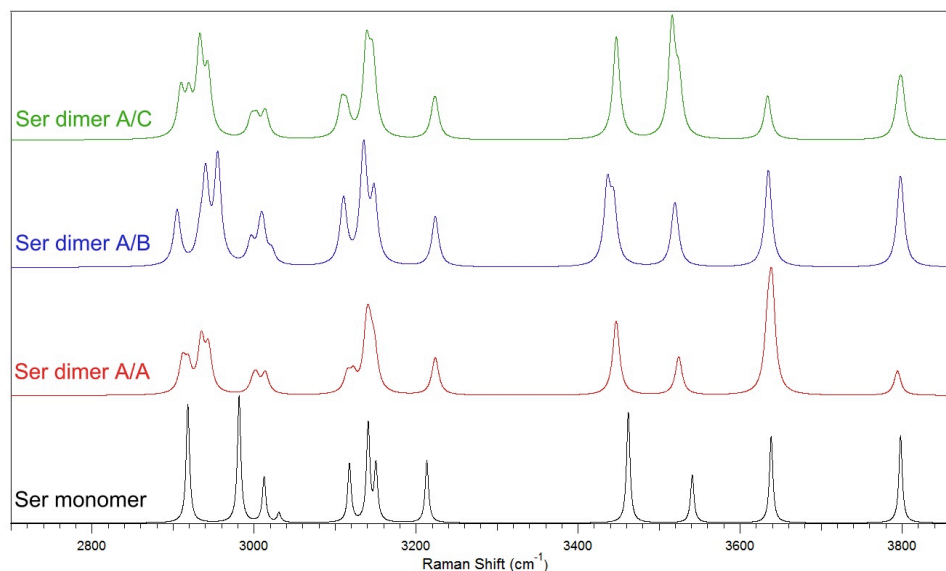
Figure 3.3.2.3: *High Frequencies of Simulated Serotonin dimer Raman Spectra*

Following the structural optimization and Raman simulation of three Serotonin dimers, the trimeric structure was studied. A crystal structure can be defined as a unit cell, composed of atoms arranged in a particular way, which is periodically repeated in three dimensions as a lattice [45]. Because of the difficulty associated with large-atom systems in computations run at B3LYP 6-311++G** level of theory, the trimer state of serotonin is the highest accumulation of atoms considered in this project. Based upon the lowest-energy conformation of the three serotonin dimer structures studied, these sites were modified to predict the favored trimeric structure. The lowest-energy conformation of the trimer is identified, as seen in **Table 3.3.2.2,** with A-A and A-C noncovalent interacting sites. A Molekel depiction of this structures is shown on the Raman spectra and is plotted alongside the optimized monomer and dimer for comparison. The serotonin trimer with A-B and A-C interacting sites was not plotted in this case because it has very similar peaks to the lowest energy conformer spectrum. It should be noted, however, that in the crystalline solid, these interacting sites would be present but are simply not seen to affect the spectrum.

Conformer	Energy (Hartrees)
Ser trimer A-A/A-C	-1719.5394443
Ser trimer A-B/A-C	-1719.5387159

Table 3.3.2.1: *HF Energies of two serotonin trimers*
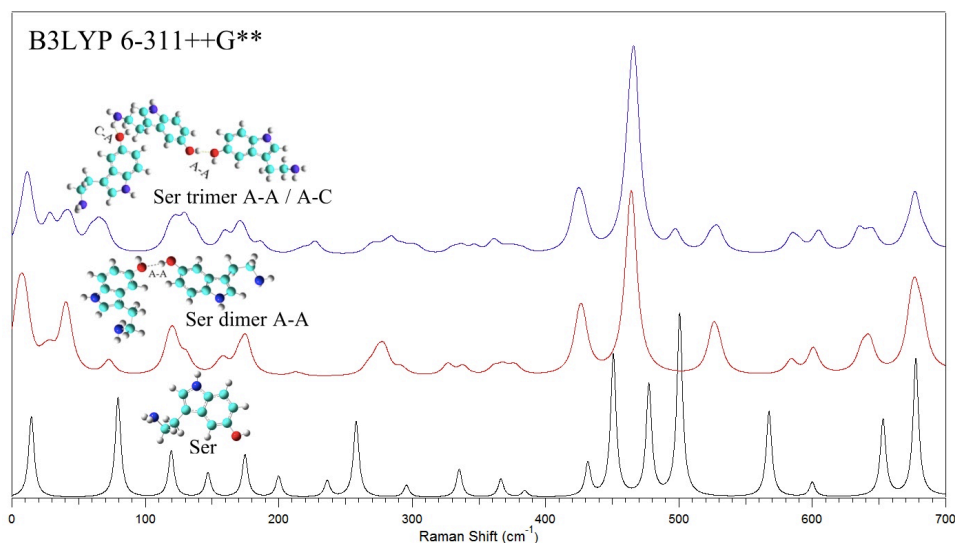
Figure 3.3.2.3: *Low Frequencies of Simulated Serotonin trimer Raman Spectra*
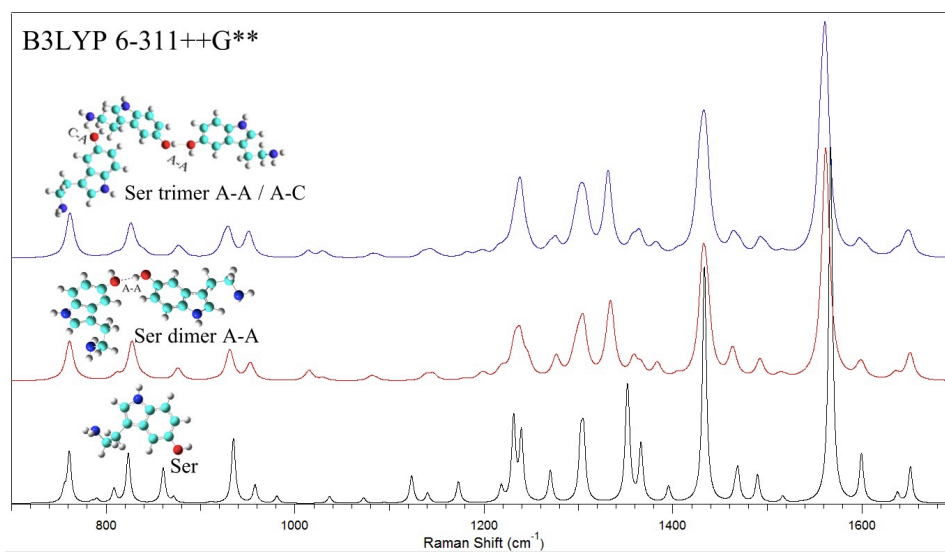
Figure 3.3.2.4: *Middle Frequencies of Simulated Serotonin trimer Raman Spectra*
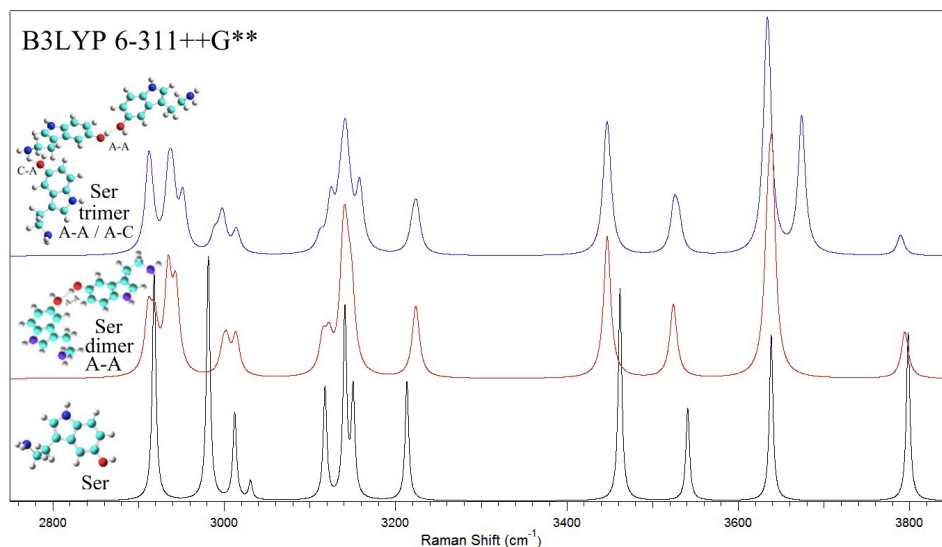
Figure 3.3.2.5: *High Frequencies of Simulated Serotonin trimer Raman Spectra*

Based upon the marked similarity between the dimer and trimer simulated Raman spectrum of serotonin, the dimer form will be carried forward as a system that compensates for the crystallization effects of serotonin. Larger crystal structures are also deemed unnecessary to be studied as far as determining their effects on the Ramana spectrum.

3.3.3 Serotonin-(Water) Clusters

As previously discussed, there are four different conformations considered in the noncovalent interactions between alcohol groups and serotonin which were provided in **Figure 3.1.1**. Following this trend, a singular water molecule was placed in these four positions, structurally optimized, and simulated under Raman spectroscopy using B3LYP 6-311++G** level of theory. The following figures provide the low and high frequency spectra combining the four conformers along with the serotonin monomer alone for comparison. Frequency shifts are visualized in important peaks of the spectra such as at 1172, 1599, and 2981 wavenumber, which correspond to O-H bending, $N-H_2$ bending, and H scissoring motions. The complete list of peak shifts is provided in **Table 3.3.3.1**, which

highlights the solvent effects of water on the Raman spectrum of serotonin based upon the location of the interactions. The Hartree-Fock energies associated with each of the structures is provided below in **Table 3.3.3.2** and help indicate where the alcohol molecules most favorably interact. The lowest energy conformer proved to be with water in the A state in relation to serotonin, with the D state conformer assuming an identical interacting position. This was expected since Oxygen is the most electronegative atom in serotonin.
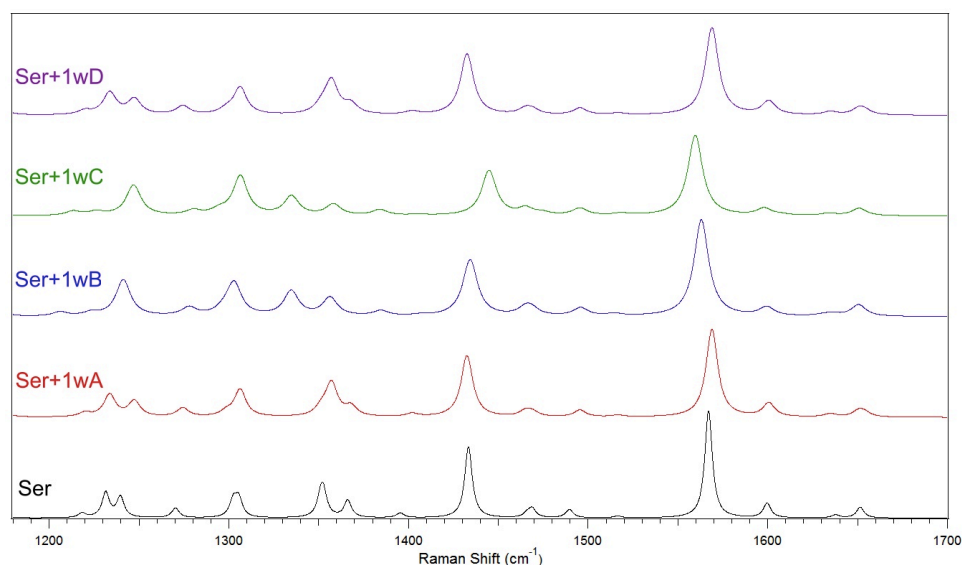
Figure 3.3.3.1: *LF of Simulated Serotonin+1H2O Raman Spectra*
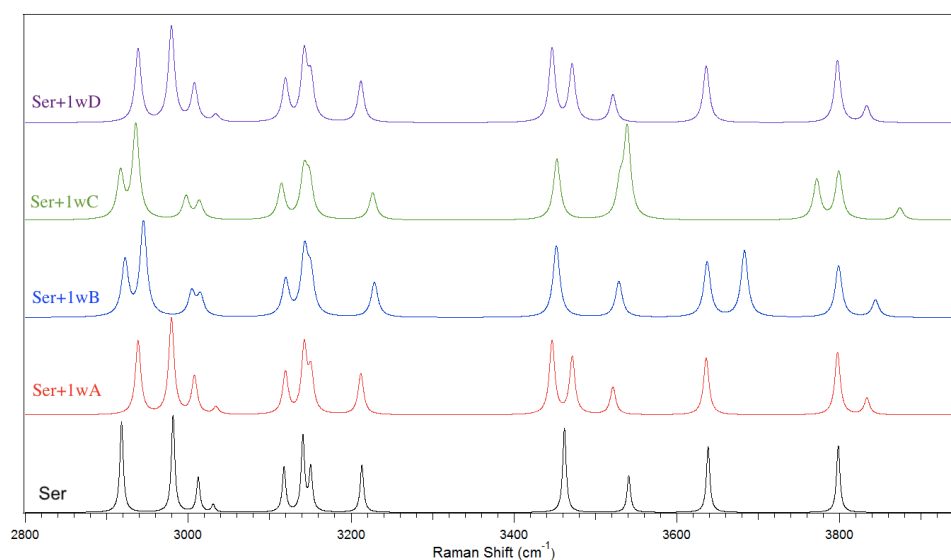
Figure 3.3.3.2: *HF of Simulated Serotonin+1H2O Raman Spectra*

ν	1wA	1wB	1wC									
1	11.7	13.9	-77.9	27	755.8	753.5	754.7	54	1402	1406	1405
2	42.5	20.2	25.7	28	763.5	763.2	763.6	55	1433	1434	1445
3	50.6	26.2	27.1	29	788	784.4	784.2	56	1465	1465	1465
4	76.1	104.6	31.3	30	814.2	809.4	805.3	57	1469	1468	1475
5	117.2	115.5	95.7	31	820.7	827.1	825.6	58	1495	1496	1495
6	129.2	119.4	102.5	32	852.3	843.3	846.7	59	1517	1515	1518
7	150.5	136.7	117.4	33	872.2	875.5	867.1	60	1569	1563	1560
8	167.8	153.7	129.9	34	875.6	882.3	878.9	61	1601	1599	1598
9	179.6	169.7	151.1	35	914.6	911.6	911.2	62	1635	1630	1607
10	233.4	219.0	165.2	36	936.8	932.2	931.9	63	1651	1635	1634
11	266.7	229	188.4	37	958.1	953.9	953.3	64	1654	1651	1651
12	278.9	261.9	221	38	1006	1017	1017	65	2939	2922	2917
13	302.8	277.1	248	39	1046	1033	1033	66	2979	2945	2936
14	346.9	294.2	256.2	40	1073	1082	1082	67	3008	3004	2997
15	369.5	345.0	307.8	41	1098	1089	1103	68	3034	3015	3014
16	380	359.5	356.2	42	1124	1139	1138	69	3119	3120	3114
17	424.5	378.1	364.8	43	1141	1148	1147	70	3142	3143	3142
18	433	423.9	421.9	44	1174	1177	1168	71	3151	3150	3149
19	452.2	432.8	434.1	45	1220	1206	1213	72	3212	3229	3227
20	478.4	462.7	463	46	1234	1223	1226	73	3447	3452	3453
21	499.5	525.6	527.2	47	1247	1241	1247	74	3471	3529	3530
22	569.6	562.2	559.7	48	1274	1278	1280	75	3521	3637	3539
23	600	587.8	600.9	49	1298	1297	1295	76	3636	3683	3772
24	651.6	605.2	639.9	50	1306	1303	1306	77	3797	3799	3799
25	678.7	646.2	674.2	51	1352	1335	1335	78	3833	3844	3874
26	731.5	678.8	685.2	52	1357	1356	1358				
				53	1368	1385	1384				

Table 3.3.3.1: *Raman Frequency Shifts dependent on Water Location*

Conformer	Energy (Hartrees)
Ser + 1wA	-649.6884151
Ser + 1wB	-649.6841894
Ser + 1wC	-649.6841882
Ser + 1wD	-649.6884152

Table 3.3.3.2: *HF Energies of the four Ser+(water)₁ Conformers*

Systems of serotonin interacting with multiple water molecules were also considered for the purpose of experimental comparison. Although the singular solvent molecule provided useful information in regards to the most favorable interaction sites to serotonin, introducing solvents into an experimental setting would result in multiple solvent molecules binding to the serotonin monomers at once. For this reason, both two

and three water molecules were structurally optimized around the monomeric system and simulated under Raman spectroscopy. The results are seen in **Figure 3.3.3.3** and **3.3.3.4**, which were calculated using B3LYP and 6-311+G** level of theory.

Figure 3.3.3.3: *LF of Simulated Serotonin+(H2O)$_{2/3}$ Raman Spectra*

Figure 3.3.3.4: *HF of Simulated Serotonin+(H2O) $_{2/3}$ Raman Spectra*

3.3.4 Serotonin-(Methanol)₁ Clusters

As previously discussed, there are four different conformations considered in the noncovalent interactions between alcohol groups and serotonin which were provided in **Figure 3.1.1**. Following this trend, a singular methanol molecule was placed in these four positions, structurally optimized, and simulated under Raman spectroscopy using B3LYP 6-311++G** level of theory. The following figures provide the low and high frequency spectra combining the four serotonin-(methanol)₁ conformer, along with the serotonin monomer alone for comparison. Frequency shifts are visualized in important peaks of the spectra such as at 1433, 1567, and 3461 cm^{-1}, which correspond to H wagging, C=C antisymmetric stretching, and N-H$_2$ stretching motions. The complete list of peak shifts is provided in **Table 3.3.4.1**, which highlights the solvent effects of methanol on the Raman spectrum of serotonin. The Hartree-Fock energies associated with each of the structures is provided below in **Table 3.3.4.2** and indicate where the alcohol molecules most favorably interact. The lowest energy conformer proved to be methanol in the A state, since Oxygen is the most electronegative atom in serotonin.
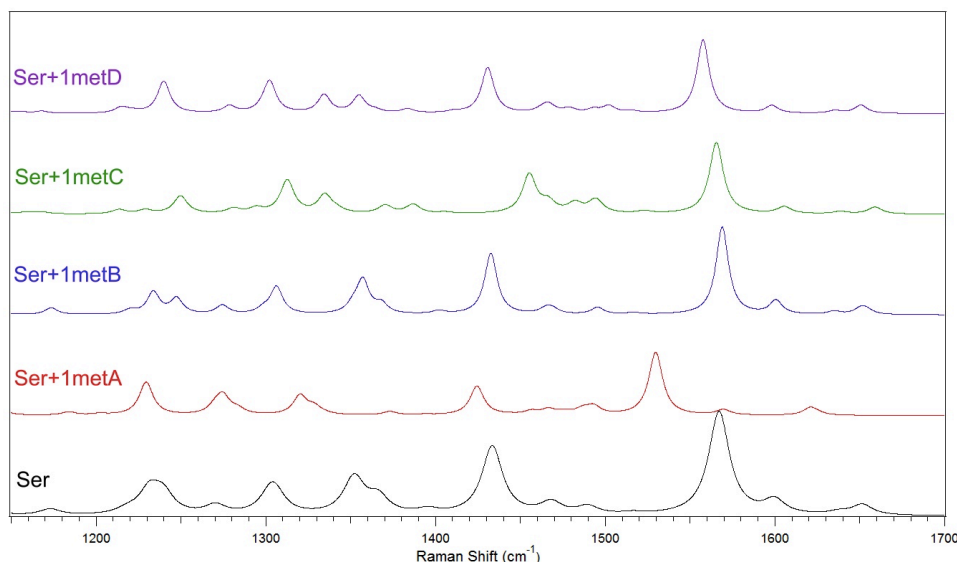
Figure 3.3.4.1: *LF of Simulated Serotonin+1met Raman Spectra*

Figure 3.3.4.2: *HF of Simulated Serotonin+1met Raman Spectra*

**Table 3.3.4.1** *Raman Frequency Shifts dependent on Methanol Location*

ν	metA	metB	metC	metD
1	26.6	10.0	15.2	14.7
2	61.7	17.8	20.9	22.3
3	84.6	25.9	29	26.7
4	98.4	26.8	39.3	32.1
5	108	69.5	52.4	54.5
6	135	106	74.5	85.4
7	140	110	109	99.6
8	148	119	119	116
9	182	137	139	128
10	183	155	161	154
11	204	170	168	168
12	237	217	221	225
13	303	219	232	261
14	326	261	272	263
15	367	294	310	297
16	374	344	325	349
17	422	362	356	356
18	431	378	365	384
19	432	424	422	422
20	444	432	431	432
21	459	463	461	453
22	528	527	526	462
23	573	587	559	526
24	602	603	595	589
25	642	604	631	606
26	659	645	676	646
27	670	678	712	680
28	743	752	741	753
29	749	763	760	763
30	762	784	779	787
31	788	809	811	809
32	805	827	827	826
33	840	843	842	846
34	859	875	852	870
35	868	883	877	879
36	911	911	899	915
37	913	932	931	933
38	924	953	953	954
39	941	1016	1016	1012
40	994	1032	1031	1030
41	1018	1049	1033	1038
42	1056	1082	1062	1079
43	1061	1088	1083	1081
44	1080	1093	1104	1089
45	1123	1139	1139	1140
46	1133	1147	1141	1151
47	1135	1158	1159	1157
48	1144	1177	1168	1167
49	1183	1206	1213	1214
50	1202	1223	1228	1221
51	1229	1241	1249	1239
52	1270	1278	1280	1278
53	1274	1296	1294	1298
54	1283	1303	1312	1302
55	1320	1334	1334	1334
56	1328	1356	1341	1354
57	1334	1384	1370	1364
58	1373	1394	1386	1383
59	1393	1406	1405	1411
60	1424	1434	1455	1430
61	1443	1460	1466	1461
62	1456	1465	1466	1465
63	1466	1468	1481	1467
64	1475	1479	1483	1478
65	1486	1493	1493	1493
66	1492	1495	1492	1502
67	1494	1514	1522	1515
68	1529	1562	1565	1557
69	1569	1599	1605	1598
70	1620	1635	1638	1635
71	1624	1650	1658	1650
72	2894	2922	2921	2922
73	2920	2944	2943	2944
74	2987	2946	2986	2959
75	2990	2986	3010	3003
76	3014	3005	3028	3004
77	3054	3015	3048	3029
78	3108	3058	3107	3064
79	3113	3119	3123	3119
80	3138	3142	3153	3142
81	3152	3149	3162	3153
82	3232	3228	3238	3230
83	3430	3452	3449	3452
84	3448	3528	3500	3530
85	3547	3637	3535	3634
86	3654	3701	3792	3711
87	3662	3799	3796	3797

Conformer	Energy (Hartrees)
Ser + 1metA	-688.7370588
Ser + 1metB	-688.9934108
Ser + 1metC	-688.8002966
Ser + 1metD	-688.9912512

Table 3.3.4.2: *HF Energies of the four Ser+(methanol)$_1$ Conformers*

Systems of serotonin interacting with multiple methanol molecules were also considered for the aim of greater compatibility with experimental data. Although the singular solvent molecule in computations provided useful information about the most favorable interaction sites to serotonin, introducing solvents into an experimental setting results in multiple solvent molecules binding to the monomers at once. For this reason, both two and three methanol molecules were structurally optimized interacting with Serotonin noncovalently and simulated under Raman spectroscopy. The results are seen in **Figure 3.3.4.3** and **3.3.4.4** and used B3LYP and 6-311+G** level of theory.
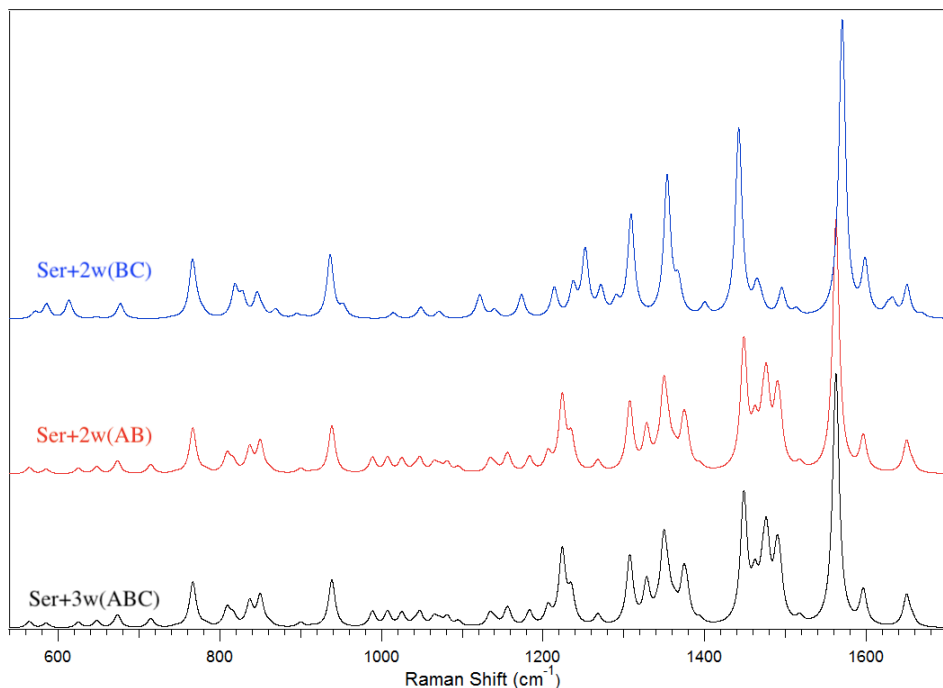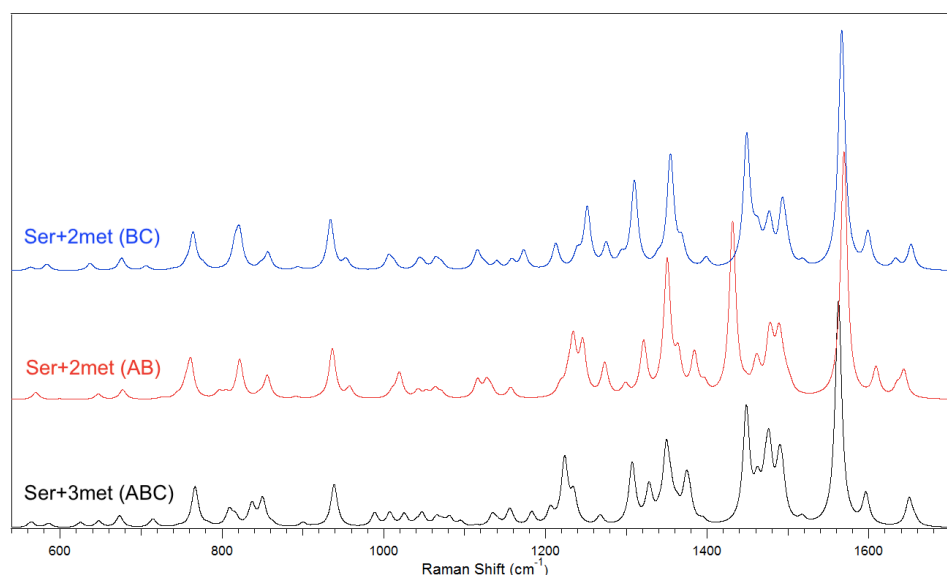

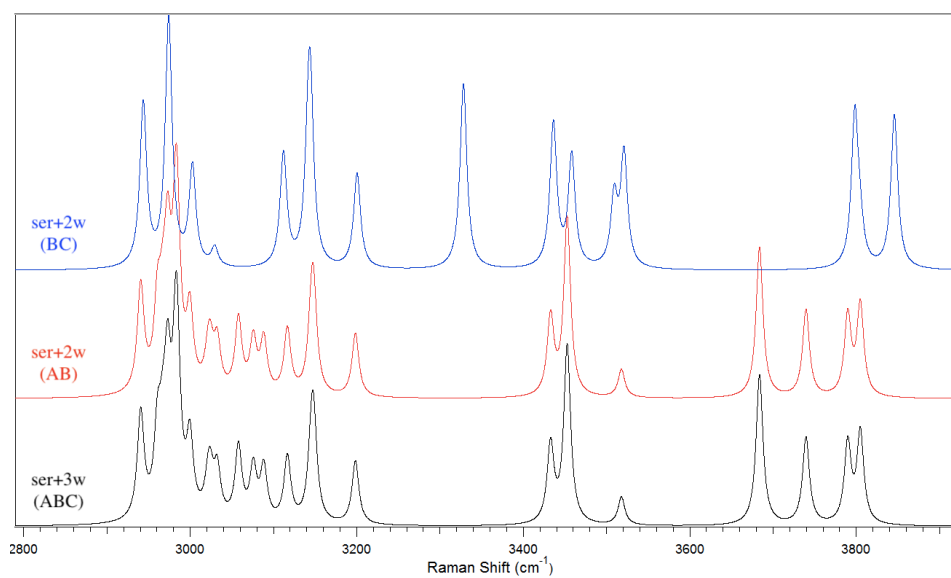**Figure 3.3.4.3:** *LF of Simulated Serotonin+(Met)$_{2/3}$ Raman Spectra*

Figure 3.3.4.4: *HF of Simulated Serotonin+(Met) $_{2/3}$ Raman Spectra*

3.3.5 Serotonin-(Ethanol)$_1$ Clusters

As previously discussed, there are four different conformations considered in the noncovalent interactions between alcohol groups and serotonin which were provided in **Figure 3.1.1**. Following this trend, a singular ethanol molecule was placed in these four positions, structurally optimized, and simulated under Raman spectroscopy using B3LYP 6-311++G** level of theory. Frequency shifts are visualized in important peaks of the spectra such as at 1231, 1305, and 3213 cm^{-1}, which correspond to benzene breathing, rocking, and N-H stretching motions. The complete list of peak shifts is provided in **Table 3.3.5.1**, which highlights the solvent effects of water on the Raman spectrum of serotonin based upon the location of the interactions. The Hartree-Fock energies associated with each of the structures is provided below in **Table 3.3.5.2** and help indicate where the alcohol molecules most favorably interact. The lowest energy conformer proved to be methanol in the A state, since Oxygen is the most electronegative atom in serotonin.

54
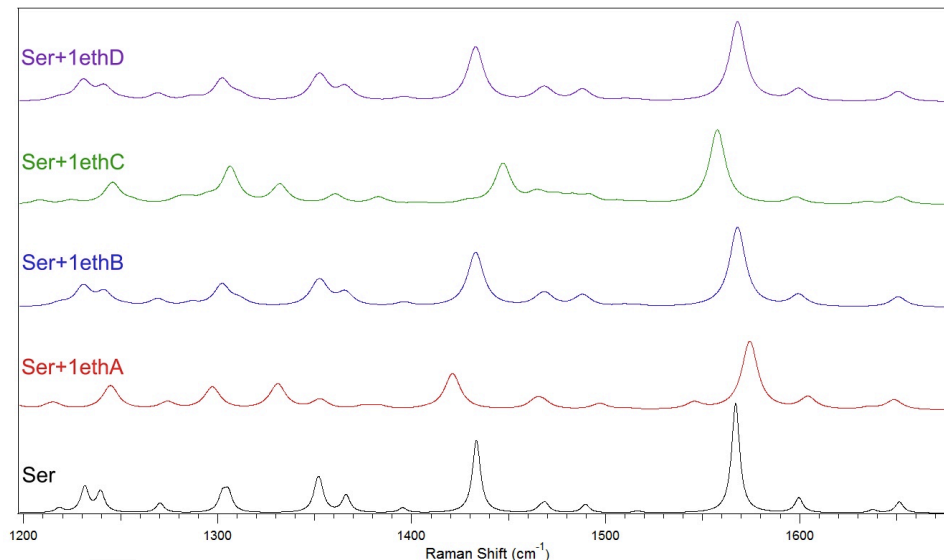
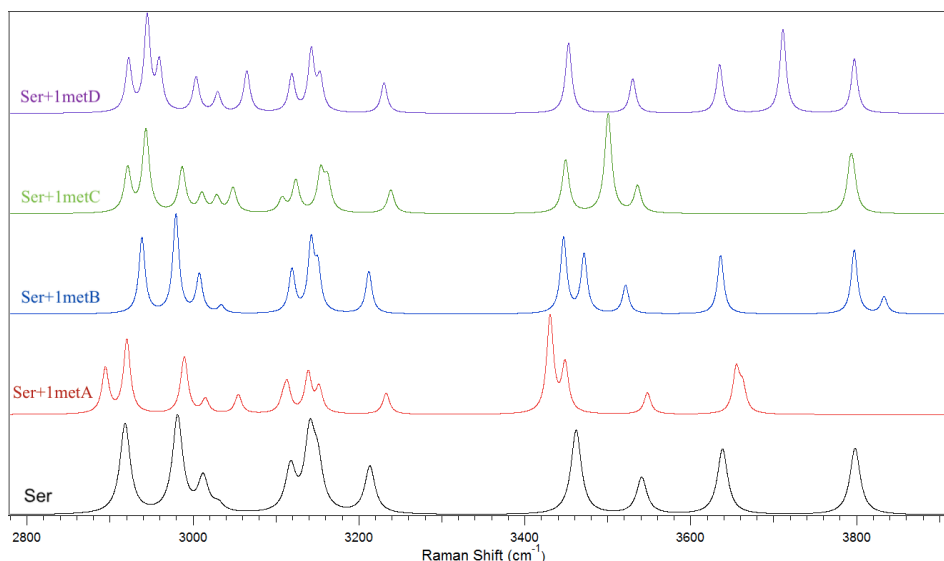**Figure 3.3.5.1:** *LF of Simulated Serotonin+1eth Raman Spectra*
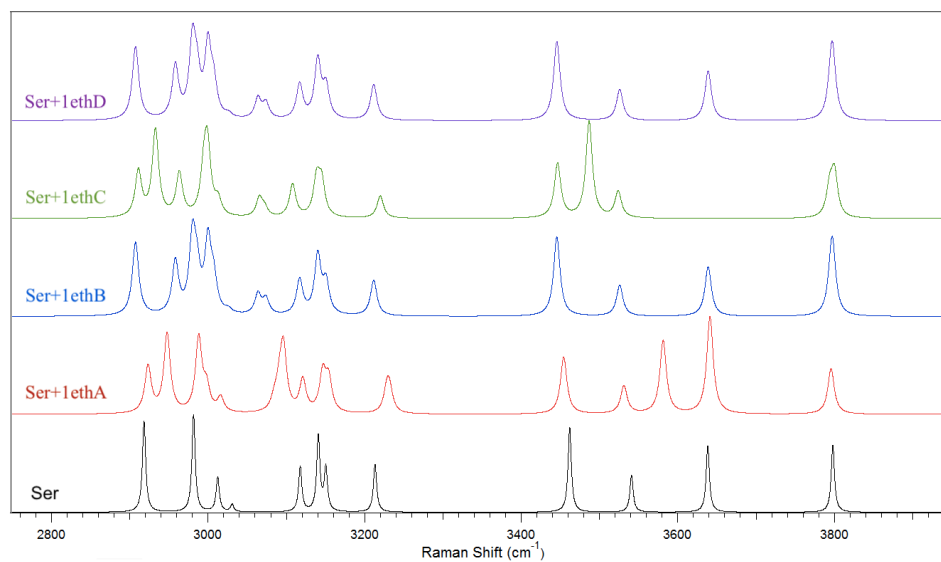
Figure 3.3.5.2: *HF of Simulated Serotonin+1eth Raman Spectra*

ν	ethA	ethB	ethC	ethD										
					10	80.4	147	158	154	**20**	273	393	414	403
1	10.8	5.75	13.4	12.6	**11**	103	176	168	168	**21**	307	417	422	422
2	16.1	13.1	17.9	17.3	**12**	112	226	186	225	**22**	355	432	428	432
3	19.3	15.1	20.8	24.5	**13**	119	251	219	261	**23**	369	452	462	438
4	21.7	32.5	27.2	31.4	**14**	129	257	247	262	**24**	422	489	526	462
5	28.1	45.1	41.2	42.2	**15**	159	290	267	263	**25**	434	499	561	526
6	33.5	55.3	59.0	63.3	**16**	165	294	299	295	**26**	442	568	595	589
7	40.1	90.3	104	87.7	**17**	184	323	308	346	**27**	464	599	634	606
8	43.7	99.1	118	115	**18**	226	334	355	356	**28**	497	652	676	646
9	75.5	124	131	127	**19**	261	368	362	382	**29**	526	677	717	679

30	582	755	741	754	**53**	1167	1218	1208	1214	**76**	1545	1599	1598	1598
31	605	761	760	764	**54**	1196	1230	1224	1221	**77**	1574	1650	1634	1635
32	644	784	773	788	**55**	1212	1241	1245	1240	**78**	1604	1651	1651	1650
33	667	806	809	797	**56**	1215	1252	1255	1271	**79**	1636	2907	2910	2921
34	678	814	811	804	**57**	1244	1269	1279	1278	**80**	1648	2958	2932	2944
35	754	816	825	826	**58**	1274	1286	1285	129	**81**	2923	2980	2963	2954
36	764	829	842	845	**59**	1296	1302	1294	1302	**82**	2947	2985	2994	2988
37	790	863	849	870	**60**	1297	1311	1306	1334	**83**	2988	2999	2997	3002
38	807	872	875	872	**61**	1325	1351	1332	1354	**84**	2998	3007	2999	3026
39	826	881	878	879	**62**	1329	1353	1360	1363	**85**	3016	3025	3012	3030
40	839	910	894	916	**63**	1330	1365	1382	1383	**86**	3084	3063	3065	3050
41	871	935	930	933	**64**	1333	1392	1390	1387	**87**	3091	3073	3072	3063
42	881	963	952	954	**65**	1352	1396	1403	1397	**88**	3096	3116	3107	3119
43	921	986	1014	1012	**66**	1375	1429	1429	1411	**89**	3096	3140	3138	3142
44	932	1020	1027	1030	**67**	1383	1433	1447	1431	**90**	3120	3150	3145	3153
45	953	1039	1031	1049	**68**	1407	1465	1463	1464	**91**	3146	3211	3219	3230
46	1015	1078	1071	1069	**69**	1421	1468	1467	1467	**92**	3154	3445	3446	3452
47	1033	1079	1080	1081	**70**	1463	1469	1474	1472	**93**	3228	3525	3486	3530
48	1072	1093	1102	1090	**71**	1464	1487	1483	1479	**94**	3232	3638	3523	3635
49	1083	1129	1136	1119	**72**	1467	1489	1491	1499	**95**	3454	3795	3794	3707
50	1085	1139	1145	1139	**73**	1496	1509	1506	1502	**96**	3531	3797	3800	3797
51	1138	1165	1161	1152	**74**	1510	1515	1518	1515					
52	1149	1173	1168	116	**75**	1545	1568	1557	1558					

Table 3.3.5.1 *Raman Frequency Shifts dependent on Ethanol Location*

Conformer	Energy (Hartrees)
Ser + 1ethA	-728.8672212
Ser + 1ethB	-728.3224917
Ser + 1ethC	-728.2782085
Ser + 1ethD	-728.3233224

Table 3.3.5.2: *HF Energies of the four Ser+(ethanol)₁ Conformers*

Systems of serotonin interacting with multiple ethanol molecules were also considered in order to obtain better matchup with experimental data. Although the singular solvent molecule in computations provided useful information about the most favorable interacting sites with serotonin, the introduction of solvent molecules into an experimental setting typically results in multiple noncovalent interactions to the monomers at once. For this reason, both two and three methanol molecules were structurally optimized interacting

with Serotonin noncovalently and simulated under Raman spectroscopy. The results are

seen in **Figure 3.3.5.3** and **3.3.5.4** and used B3LYP and 6-311+G** level of theory.

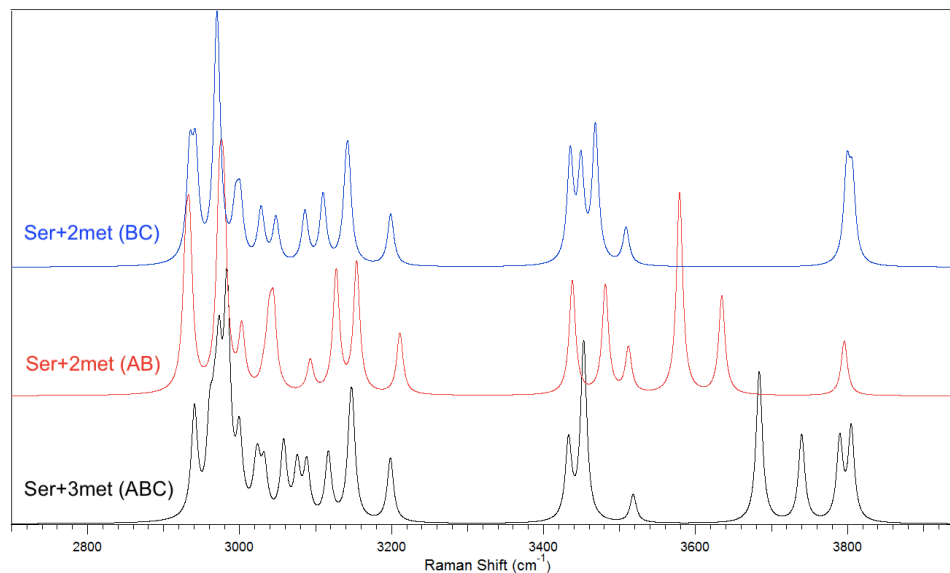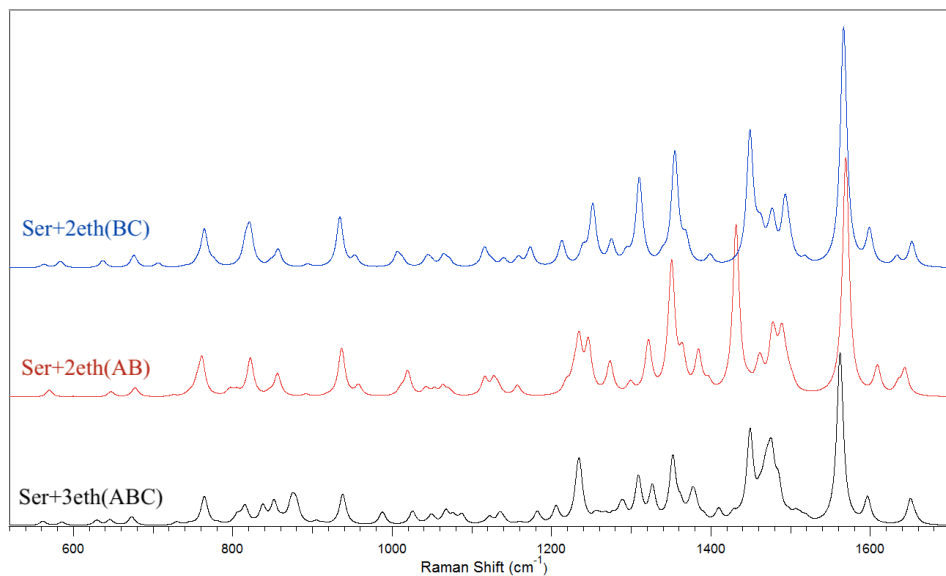**Figure 3.3.5.3:** *LF of Simulated Serotonin+(Eth)$_{2/3}$ Raman Spectra*
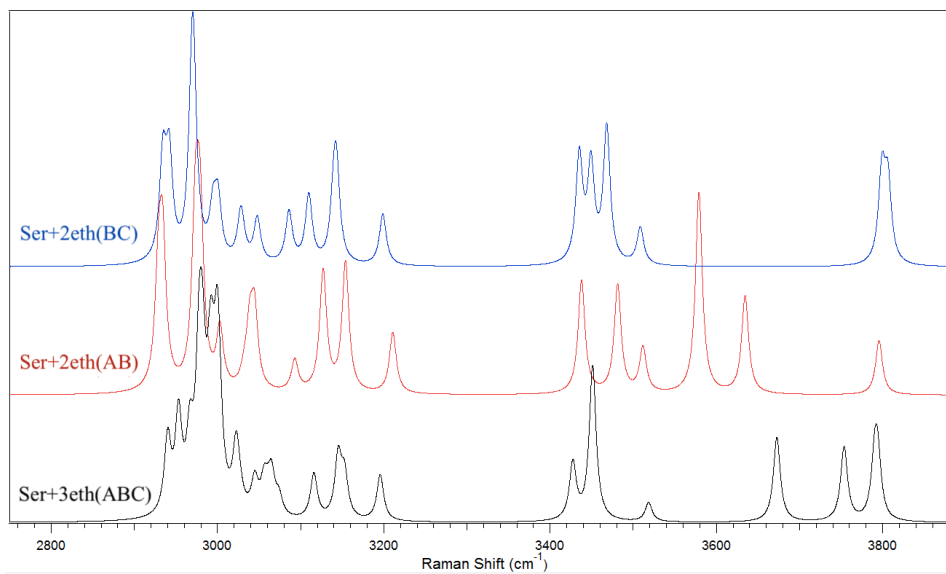
Figure 3.3.5.4: *HF of Simulated Serotonin+(Eth)$_{2/3}$ Raman Spectra*

57

Chapter 4: Experimental Methods

4.1 Instrumentation

The primary instrument used for the experimental data collection portion of this research was a Horiba HR Evolution Raman Spectrometer as shown in **Figure 4.1**. The excitation sources used to obtain experimental spectra were a Nd:YAG 532nm laser and 633nm laser with ultralow frequency capability, which were restricted in output power based upon the system. The green 532nm laser was always initially used because it is the most powerful laser available and provided optimal scattering with lowest fluorescence observed for the systems being investigated. The objectives varied between 10x, 50x, and 100x, and were selected based upon the optimal signal: noise ratio observed in the sample.

Figure 4.1: *Image of the Horiba HR Evolution Raman Spectrometer, image taken from: https://www.horiba.com/en_en/products/detail/action/show/Product/labram-hr-evolution-1083/*

4.1.1 Calibration

Each day before any experimental data was collected, the Raman spectrometer was calibrated, which typically took less than five minutes total. This process begins with turning on only the green 532nm laser channel, and then a calibration slide containing a

sample of a silicon wafer is placed on the stage of the spectrometer. Next, a CCD camera is used to find the sample on the slide, and a 10x objective lens is used to obtain the calibration spectra. A joystick is used during these processes for fine movements in order to obtain a clear image of the silicon wafer or sample being investigated. Once the silicon wafer is detected on the calibration slide using the CCD camera and crosshairs on the computer screen, the Raman is then ready to calibrate. The autocalibration is carried out using the parameters of a 532nm laser and a 600gr/mm grating, which results in the establishment of a zero-point and the vibrational peak associated with the silicon wafer at approximately 520cm^{-1}. Once these two peaks are identified, the instrument is successfully calibrated and ready to collect data.

4.2 Sample Preparation

One of the greatest advantages to using a Raman spectrometer is the little sample preparation needed in order to collect experimental data. Once appropriated on a glass slide or well, a solid or liquid material can be investigated as is. The Serotonin was purchased from Sigma-Aldrich, appearing as a white crystalline solid, and was not further purified.

For the monomeric collection, a miniscule amount of solid was focused using the objective microscope and signal: noise ratio optimized using the focus, stage movements, and altering the laser power, acquisition time, accumulations, and grating parameters. The optimized parameters are noted for each spectrum obtained.

In order to study the solvent-interactions spectroscopically, a custom Raman setup was used involving a vacuum chamber adapted from a previous thesis project in the Hammer group [46]. An image of the system is shown below in **Figure 4.2.1** and consists of a vacuum system with Teflon tubing, a sample chamber with gauges for sealing that

rests below the microscope objective, and a solvent chamber with heating wire requiring output voltage to assist in vaporization. A schematic diagram indicating the flow of the solvent through the chamber is provided in **Figure 4.2.2** and provides a closer look of the sample and solvent interaction chamber. The foundation of this setup is to introduce solvent vapors to the solid sample and the heating apparatus is added in order to lower the vapor pressure of the solvent, according to the Ideal gas law, and promote gaseous flow.

Figure 4.2.1: *Image of Custom Raman spectroscopy setup*
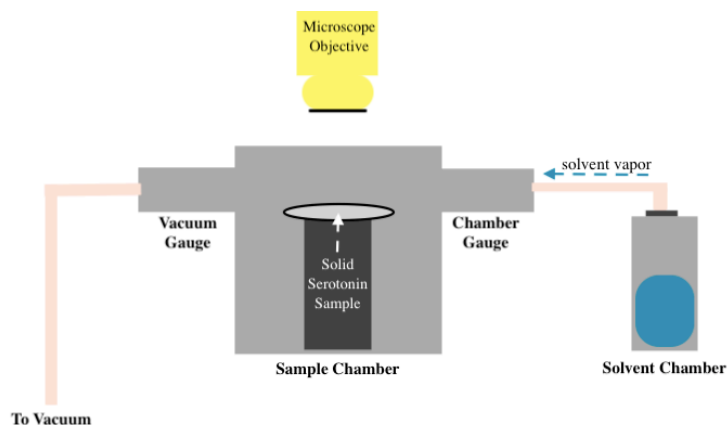
Figure 4.2.2: *Schematic Diagram of Custom Raman spectroscopy setup*

The solvent was placed into the sealed metal chamber, heated and vaporized using the output power system, and assisted through the system by the vacuum. After heating for approximately five minutes in the sealed chamber, the two gauges were opened to allow free flow through the system and avoid solvent condensation on the glass. Once this system was flowing properly for an additional five minutes, the serotonin sample was focused on the microscope stage and the Raman data finally collected.

4.3 Data Collection
4.3.1 Serotonin Solid

The following spectra were collected using a 633nm laser with 100% power, 50x objective, an 1800 grating, 5 second acq. time, 20 accumulations, and applying the denoise filter. The spectrum was processed using a baseline subtraction and peaks identified with at least 3 times the baseline at the wavenumber at which the signal came to an apex. Our laboratory is also capable of gathering high resolution data at ultralow frequencies using a specialty filter, and these results are provided for both using the ULF filter and not.
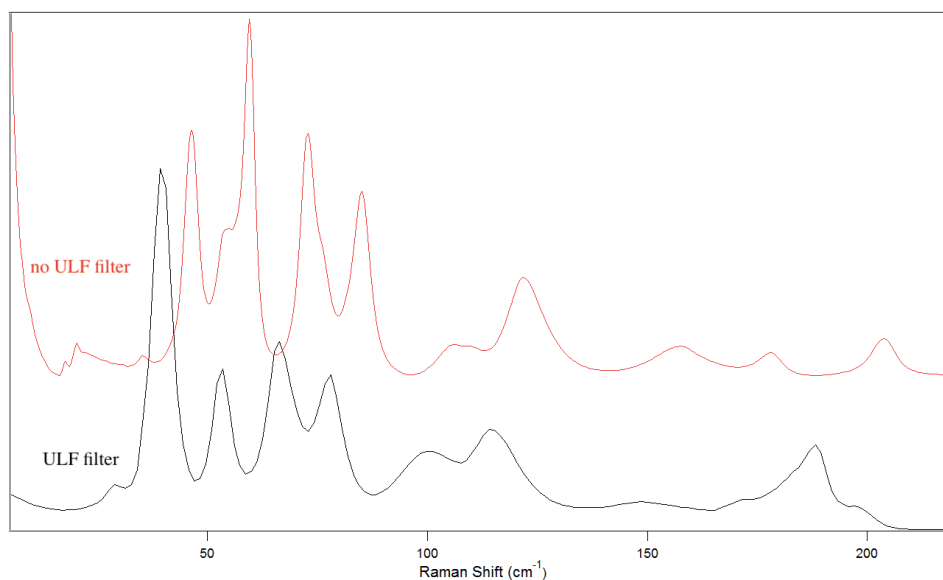
Figure 4.3.1.1: *ULF Serotonin Raman Spectrum with 633nm Excitation source*

The comparison of peak intensity between using the ULF filter and not is so similar that it negates the necessity of using the filter piece in subsequent data collection. The observed experimental peaks for the serotonin solid are provided in **Table 4.3.1** and compared to both theory and a reference spectrum of serotonin previously published [37]. There is excellent matchup between our experimental data and that which was previously published by the Omkant group, with our spectra resulting in greater matchup with theory.

Figure 4.3.1.2: *LF Serotonin Raman Spectrum with 633nm Excitation source*

Figure 4.3.1.3: *HF Serotonin Raman Spectrum with 633nm Excitation source*

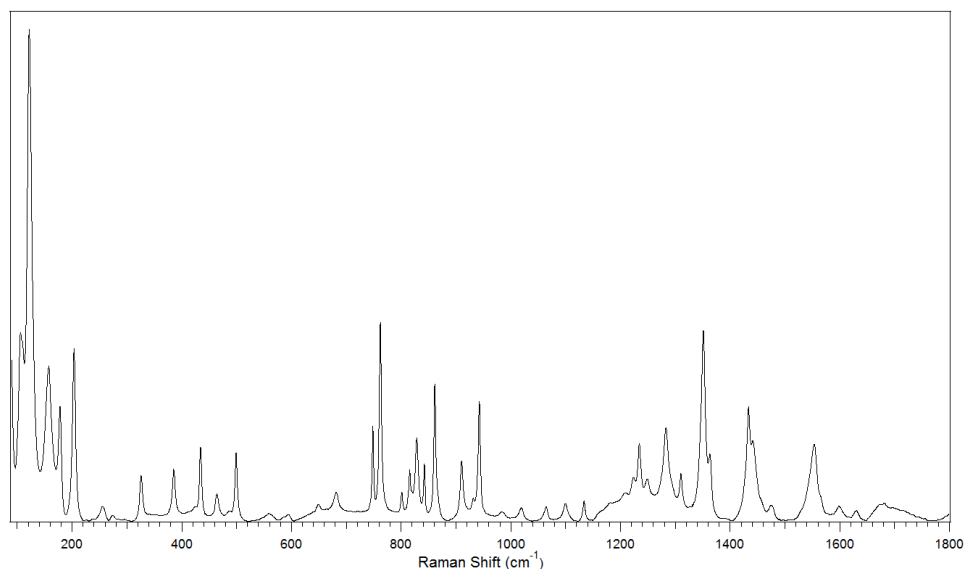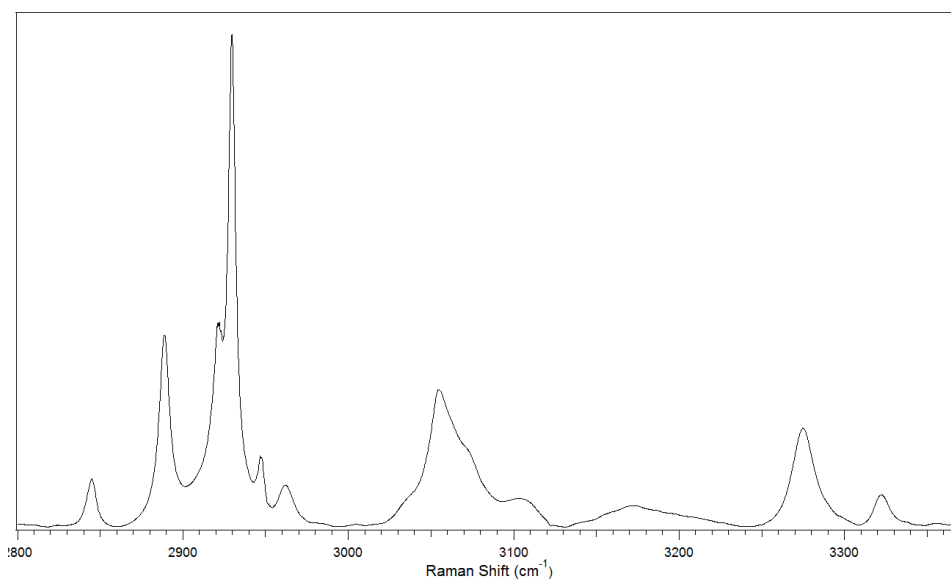| Mode (ν)	Obs. (cm⁻¹)	Theory (cm⁻¹)	Ref. (cm⁻¹)
1	28.9	14.5	66
2	78.1	79.5	76
3	114.1	119.4	102
4	148.6	146.9	151
5	171.6	174.6	198
6	197.1	199.8	-
7	248.9	236.2	249
8	267.7	258	-
9	-	295.6	-
10	320.3	335.2	319
11	-	366.4	-
12	380	384.3	379
13	428.2	431.6	-
14	460.1	450.8	427
15	480.8	477.4	458
16	499	500.5	491
17	557.7	567.4	588
18	587.4	599.9	-
19	643.7	653	643
20	677	677.5	-
21	757.4	755.5	741
22	762	761	755
23	-	785	-
24	796	790.2	795
25	810	808.4	809
26	824	823.5	822
27	856.5	860.5	836
28	861.3	871.5	854
29	910.2	910.9	904
30	931.3	934.8	935
31	942.4	957.6	978
32	983	980.7	1013
33	1019	1036	1055
34	1064	1072	-
35	1099	1094	1092
36	1127	1123	1126
37	1133	1140	-
38	1178	1172	-
39	1218	1218	1203
40	1229	1231	1227
41	1242	1239	1240
42	1278	1270	1275
43	-	1302	1303
44	1306	1305	-
45	1351	1351	1343
46	1358	1352	1355
47	1362	1366	-
48	1395	1395	1426
49	1433	1433	1437
50	1470	1466	1466
51	1474	1468	-
52	-	1489	1514
53	1553	1516	-
54	1563	1567	1546
55	1599	1599	-
56	1630	1637	1584
57	1671	1651	1587
58	2918	2918	-
59	2990	2981	2882
60	3015	3012	2924
61	3029	3030	2938
62	3104	3117	3029
63	3138	3140	3051
64	3152	3150	3066
65	3204	3213	3102
66	3274	3461	3269
67	-	3540	-
68	-	3638	-
69	-	3798	-

Table 4.3.1: *Experimental Peak Values compared to literature and a reference*[37]

4.3.2 Serotonin-Methanol Solvation

Using the custom Raman setup shown in **Figure 4.2.1**, the following spectra were collected using serotonin powder, lab grade methanol, and a 532nm excitation source with 10% laser power. The best spectra were obtained by allowing the methanol to be heated by the output source for 10 minutes prior to introduction to the sample chamber. Upon opening up the sample and vacuum gauges, methanol was pulled through the system for an additional 10 minutes to promote its interaction with serotonin. Peak frequencies are provided in **Tables 4.3.2.1-3** and are listed beside pure serotonin peak values. All three spectra, low, middle, and high frequencies, demonstrate strong signal detection and satisfactory S:N ratios. The greatest peak shifts were seen at 980, 1205, and 3419 cm⁻¹, which is similar to what the theoretical portion of this experiment predicted.
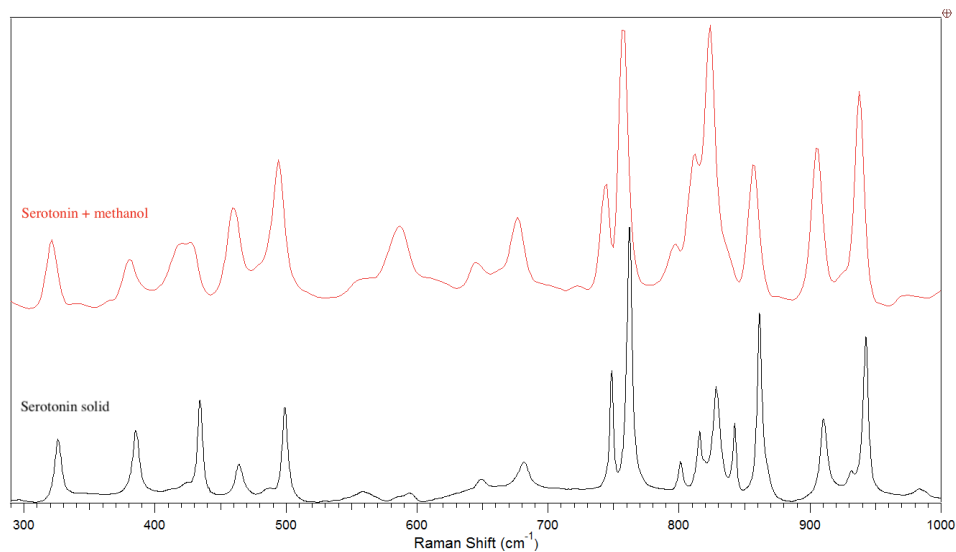
Figure 4.3.2.1: *Low Frequencies of Ser vs Ser+methanol Raman Spectrum*

Ser (cm⁻¹)	Ser+ Met	Shift (cm⁻¹)	ΔE		Ser (cm⁻¹)	Ser+ Met	Shift (cm⁻¹)	ΔE
251.5	250	1.5	R		721.5	722.54	-1.04	B
364.15	362.8	1.35	R		745.18	744	1.18	R
381.89	380.8	1.09	R		758.79	756.61	2.18	R
415.92	419.12	-3.2	B		797.81	797.31	0.5	R
428.28	427.8	0.48	R		813.03	812.19	0.84	R
461.75	459.11	2.64	R		824.85	824.01	0.84	R
495.08	494.21	0.87	R		836.65	839.18	-2.53	B
559.63	558.76	0.87	R		858.52	856.01	2.51	R
646.08	644.06	2.02	R		878.67	878	0.67	B
678.03	676.71	1.32	R		907.12	904.62	2.5	R
					937.95	937.3	0.65	R
					981.15	972.21	8.94	R

Table 4.3.2.1: *Low Frequency Peak Shifts of Ser vs Ser+methanol*

64
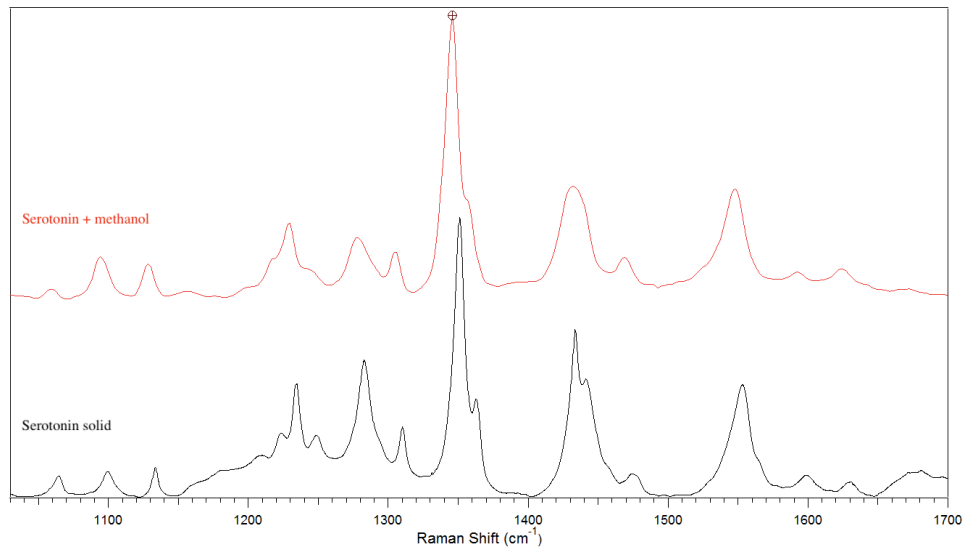
Figure 4.3.2.2: *Middle Frequencies of Ser vs Ser+methanol Raman Spectrum*

Ser (cm^{-1})	Ser+Met (cm^{-1})	Shift (cm^{-1})	ΔE		Ser	Ser+Met	Shift	ΔE
1014.2	1011.9	2.3	R		1229.8	1228.2	1.6	R
1060.3	1059.9	0.4	R		1280	1278.8	1.2	R
1095.2	1094.3	0.9	R		1306	1304.3	1.7	R
1129.4	1128.6	0.8	R		1387	1394.7	-7.7	B
1158.7	1157	1.7	R		1432	1432.5	-0.5	B
1178.2	1176.5	1.7	R		1471.3	1468.6	2.7	R
1207.3	1200.8	6.5	R		1549.2	1548.5	0.7	R
					1590	1592.3	-2.3	B
					1624.4	1623.1	1.3	R

Table 4.3.2.2: *Middle Frequency Peak Shifts of Ser vs Ser+methanol*
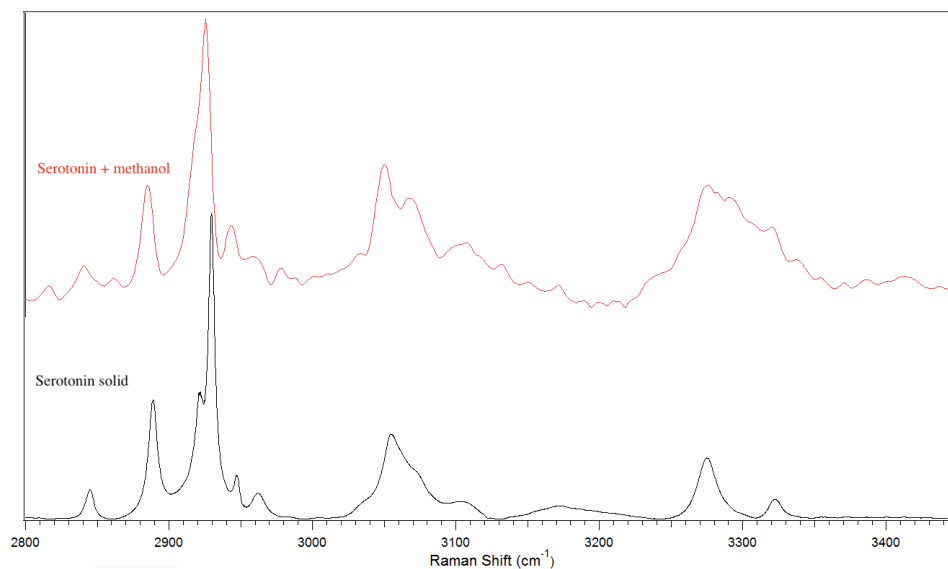
Figure 4.3.2.3: *High Frequencies of Ser vs Ser+methanol Raman Spectrum*

65

Ser (cm^{-1})	Ser+Met (cm^{-1})	Shift (cm^{-1})	ΔE		Ser	Ser+Met	Shift	ΔE
2821.8	2816.7	5.1	R		3067.3	3067	0.3	R
2844.2	2840.5	3.7	R		3108.3	3107.9	0.4	R
2869.3	2861.2	8.1	R		3240.6	3241	-0.4	B
2886.4	2884.9	1.5	R		3275.7	3276	-0.3	B
2926.7	2925.5	1.2	R		3293.1	3290.9	2.2	R
2945	2943.8	1.2	R		3317.4	3320.8	-3.4	B
2960.7	2959.3	1.4	R		3337.2	3336.9	0.3	R
3051.9	3050.2	1.7	R		3419.7	3413.5	6.2	R
					3859.1	3852.2	6.9	R

Table 4.3.2.3: *High Frequency Peak Shifts of Ser vs Ser+methanol*

Chapter 5: Data Analysis

5.1 Solid Phase: Experiment versus Theory

One of the most important steps as a chemist is confirming that your theoretical experiments match up to data collected in the laboratory. This step ultimately helps determine whether or not the project was successful, especially if the molecule has scarcely been studied. The first portion of this experiment dealt with using B3LYP 6-311++G** level of theory to determine the optimized structure for the serotonin monomer and various intramolecular dimers, and the results were used to simulate their Raman spectra. The second portion aimed to collect the highest resolution spectrum of serotonin ever taken and over the greatest wavenumber range. The following spectra attempt to confirm that our experimental spectra, collected on multiple occasions and using different parameters, match up excellently not only to each other but also with our quantum calculations.
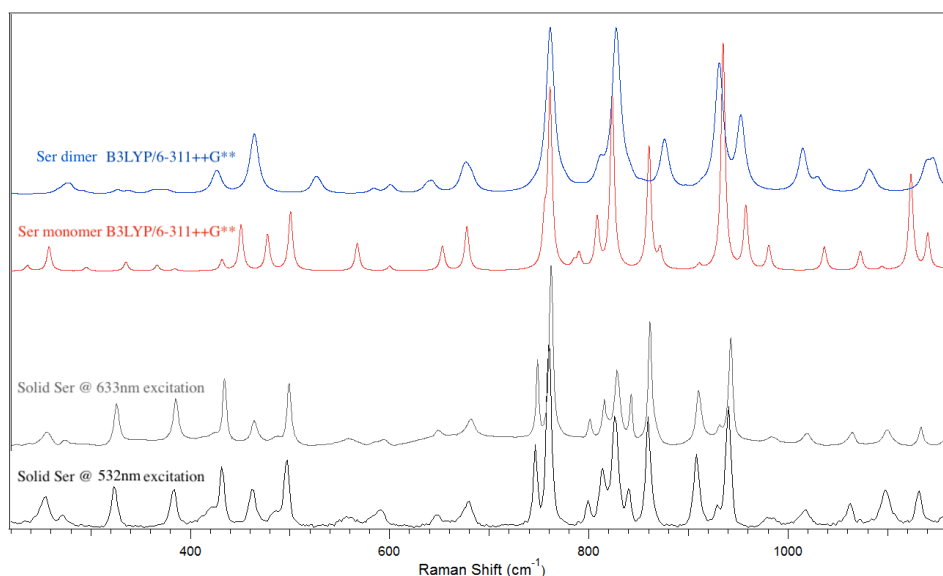
Figure 5.1.1: *Low Frequencies of Serotonin Raman Spectrum*
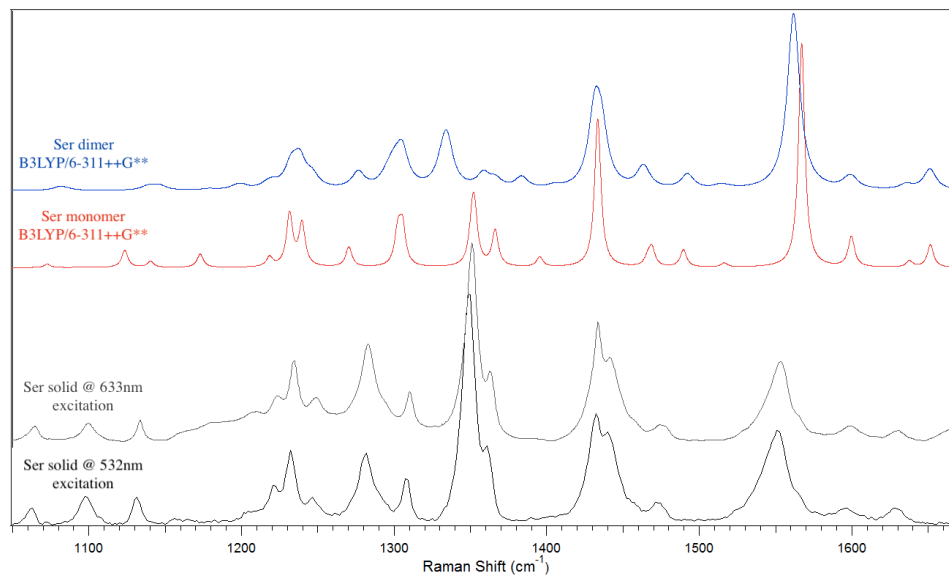
Figure 5.1.2: *Middle Frequencies of Serotonin Raman Spectrum*
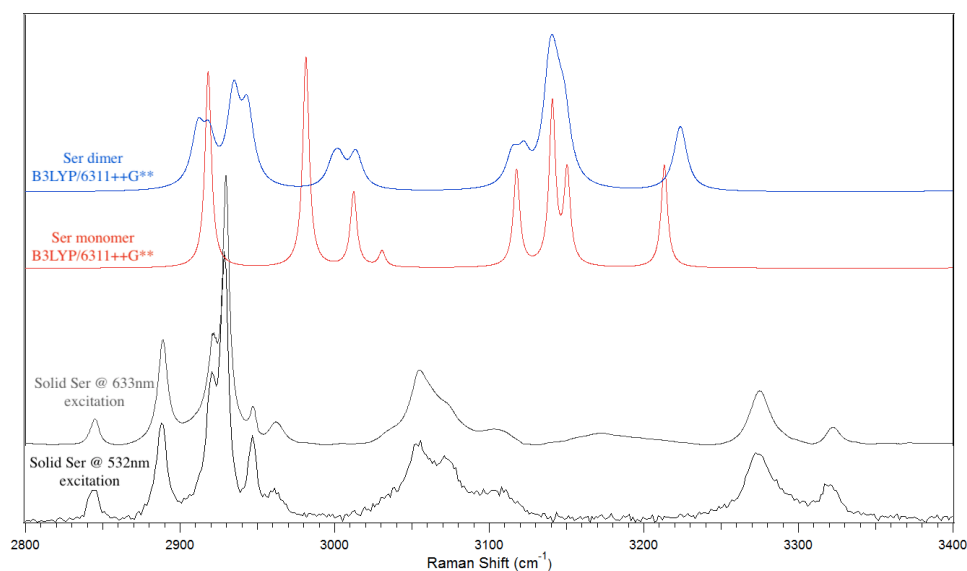
Figure 5.1.3: *High Frequencies of Serotonin Raman Spectrum*

Based upon these three portions of the Raman spectrum of Serotonin, it can be confidently said that the two experimental excitation sources lead to nearly identical results. With the best spectra, which used a 633nm excitation source, there were more peaks matched up to monomeric theory than has ever been published in the past. This is most likely due to the fact that our laboratory has ultralow frequency and high-resolution

capabilities that clarified some of the smaller peaks from background noise. The most questionable region remains to be the peaks observed above 3000 cm^{-1}, which ultimately do not match peak-for-peak with the monomeric theory. With the lowest-energy dimer state of serotonin considered, however, the peak matchups can be visualized to a much greater extent. Considering serotonin appears as a crystalline solid to the eye, this confirms our suspicion that the molecule most likely exists as a crystal at room temperature.

5.2 Serotonin-Methanol Interactions: Experiment versus Theory

Due to the uncertainty in knowing how many solvent molecules are interacting with serotonin at once in an experimental setup, it is difficult to choose a molecular model of the system. Based upon serotonin's high solubility in the organic solvent methanol, it can be assumed that, when the vapor is introduced into the system, it favors interaction at several sites at once. For this reason, the simulated spectrum with three methanol molecules noncovalently interacting with serotonin was used in comparison with experimental Raman data collected. The peak values observed for both spectral regions are shown in **Table 5.3**.
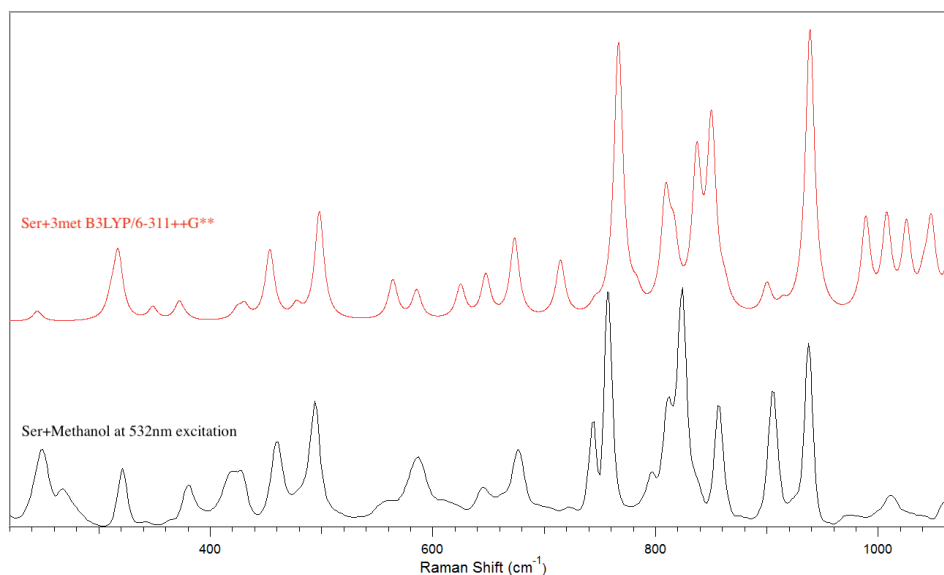
Figure 5.2.1: *Low Frequencies of Ser+methanol vs Ser+3met Raman Spectrum*

Theory (cm^{-1})	Exp. (cm^{-1})	Theory	Exp.	Theory	Exp.
244.4	247	766.4	757	1206.7	1199.2
317	321.3	780.3	797.3	1223.5	1229.8
347.7	342	815	812.2	1234.5	1242.7
372.2	380	837	824	1268	1277.2
424	421	861	856.5	1307.4	1304.3
430	427	901	905	1328.1	
453.6	459	938	937.3	1349.7	1345.7
478	481	988	972.21	1374.5	1356.8
498	495	1007.2	1011.9	1393	1392
564	558.8	1025		1448.5	1432.5
585.5	587	1047.4	1040.2	1462.2	
625	611.3	1066	1059.9	1476	1468.6
647.4	646	1081.3	1078	1490	1488
673.22	676	1094.8	1094.3	1517.3	1508
714.5	722	1114.4		1562.3	1548.5
747	744.5	1134.7	1128.6	1596.1	1593
		1156	1155.4	1650	1624.6
		1183.1	1176.5		

Table 5.2.1: *Comparison of theory vs experiment for Ser+Met Low Raman Frequencies*

The theoretical and experimental peaks of the fingerprint region match up very well, with an average +/- 2.47 cm^{-1} shift observed. Because the low frequency region is, for the most part, unique to all systems, it can be assumed that the custom Raman spectrum setup was successful in capturing the interaction of serotonin and methanol.
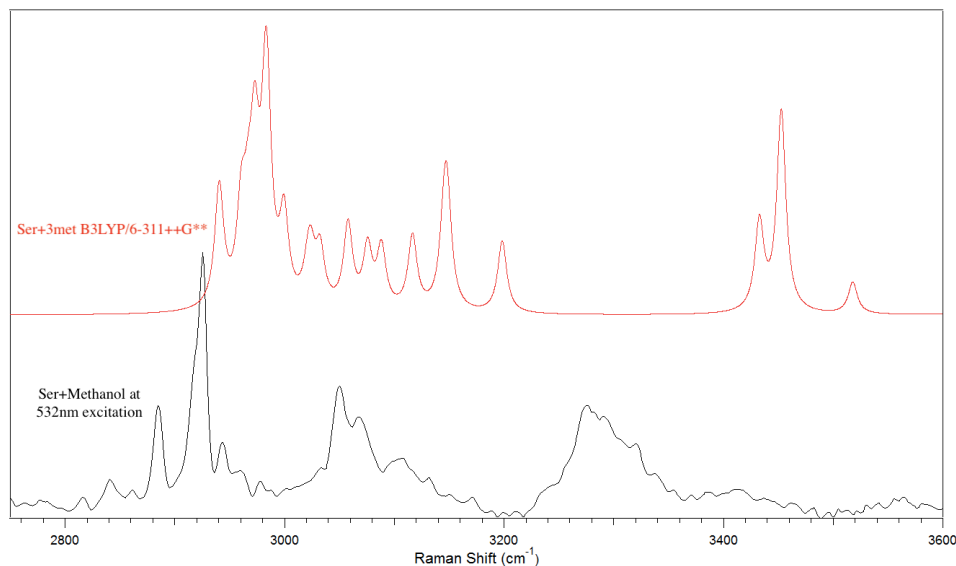

Figure 5.2.2: *High Frequencies of Ser+methanol vs Ser+3met Raman Spectrum*

Theory (cm⁻¹)	Exp. (cm⁻¹)				
2941	2884.9	3032.3	3050.2	3452.6	
2961.3	2925.5	3058.2	3067	3518	3562.4
2973.3	2943.8	3076	3108	3683.9	
2983.4	2959.3	3088	3171.9	3739.3	
3000	2978.8	3116.8	3276	3789.5	
3023.3	3033	3147.1	3290	3804.5	3852.2
		3198.4	3319.5		
		3432.4	3412.3		

Table 5.2.2: *Comparison of theory vs experiment for Ser+Met Low Raman Frequencies*

Although the higher frequency region does not demonstrate as great of a matchup with theory as seen in the fingerprint region, this is in alignment with most Raman spectrum of systems containing serotonin. The region above 3200 cm⁻¹ differs from theory in all previous publications, and this data was successfully compared with the serotonin solid spectrum. The matchup with the solid even highlighted several peak shifts present, which are key in confirming the visualization of methanol interacting with serotonin. Between excellent matchup in the fingerprint region and peak shifts noted from the serotonin solid system throughout the spectra, this also ultimately confirms our group's success in observing the solvent effects of methanol as visible in the Raman spectrum of serotonin.

Chapter 6: Conclusions

Serotonin, or 5-hydroxytryptamine, is a neurotransmitter and metabolite involved in the cardiovascular, gastrointestinal, and nervous systems. There currently does not exist a method to directly measure or detect concentration of serotonin in the human body, which presents a problem when studying diseases that involve serotonergic pathways. Raman spectroscopy presents a unique method to vibrationally characterize molecules based upon the inelastic scattering of light, and serotonin's amphipathic structure presents 69 vibrational modes that are Raman active. Using B3LYP method and 6-311++G** basis set, the optimized structures of serotonin and the lowest-energy intramolecular dimer and trimer were determined in order to help better understand the crystalline solid that exists in nature. The optimized results were simulated under Raman spectroscopy for matchup to experiment. Experimental spectra were collected for the crystalline solid using a Horiba LabRAM spectrometer, 633nm excitation source, and over the 5-4000cm^{-1} range, which has ultralow frequency and very high-resolution capabilities. The theory versus experiment comparison lead to greater peak matchup than ever previously published of the Raman spectrum of serotonin. Because of its amphipathic nature, it is also interesting to consider interactions amongst serotonin with various solvents, including both aqueous and organic. Using the same level of theory, Raman systems were modeled for serotonin and solvent molecules of water, methanol, and ethanol. The theoretical results were studied to predict the red and blue peak shifts that would be observed in experiment. Experimental spectra were collected with a custom Raman setup that vaporizes the solvent and assists in its

constant flow through the system by vacuum. The Horiba LabRAM spectrometer was again used, but with a 532nm excitation source and collected over the 200-4000cm^{-1} range. The custom setup was used to compare spectra of serotonin solid alone with data collected using the flow of methanol through the system. Because the collection of experimental data involving ethanol and water solvents was not achieved, these solvent effects were only carried out using theory. The comparison of theory with experiment of the Raman spectra of serotonin and methanol lead to the successful observation of the solvent effects that methanol has on serotonin.

Chapter 7: Future Work

Due to COVID-19 pandemic, the completion of the work originally aimed for in this thesis was cut short. Although the solid serotonin portion of the experiment was thoroughly covered, the solvent effects were not studied to the extent that this project intended. Once the outbreak ceases and chemists return to normal working hours, the Raman spectrum of serotonin interacting with ethanol and water will be collected using the custom setup that was described in this project. Once finished, the simulated data can be compared to experiment in a similar way was carried out for the serotonin and methanol system and this project altered for publication.

References

1. Atkins, Peter W. "Chemical Bonding." *Encyclopedia Britannica*. Print.
2. Piela, Lucjan. "Intermolecular Interactions." *Ideas of Quantum Chemistry. Ed.* Amsterdam: Elsevier, 2007. 681-761. Print.
3. Kuhn, Lester P. "The Hydrogen Bond. I. Intra- and Intermolecular Hydrogen Bonds in Alcohols." *Journal of the American Chemical Society.* 74.10 (1952): 2492-99. Print.
4. Das, V M. "Red shift and Blue shift." *Journal of Research & Method in Education.* 5.6 (2015): 77-101. Print.
5. Wright, A.M., et al., "Charge Transfer and Blue Shifting of Vibrational Frequencies in a Hydrogen Bond Acceptor." *The Journal of Physical Chemistry.* A, 2013. 117(26): p. 5435- 5446.
6. Lodish, H.; Berk, A.; Zipursky, S.L. "Molecular Cell Biology: Section 21.4 Neurotransmitters, Synapses, and Impulse Transmission" *NCBI*. New York: W. H. Freeman, 2000. Web.
7. Snyder, S. H., and R. B. Innis. "Peptide Neurotransmitters." *Annual Review of Biochemistry* 48.1 (1979): 755-82. Print.
8. Nelson, D.L. and M.M. Cox, "Lehninger Principles of Biochemistry." 6 ed. 2013, New York: W. H. Freeman. Print.
9. Riddle DL, Blumethal T, Meyer BJ, et al. *Section II, Neurotransmitter Metabolism and Function*. Ed. II, C. elegans. Cold Spring Harbor, NY: Cold Spring Harbor Laboratory Press, 1997. Print.
10. "Synthesis and Storage of Neurotransmitters." *Web.williams.edu*, Williams College Neuroscience, 1998, https://web.williams.edu/imput/synapse/pages/I.html.
11. Purves D, Augustine GJ, Fitzpatrick D, et al. *Neurotransmitter Release and Removal*. Neuroscience. Sunderland, MA: Sinauer Associates, 2001. Print.
12. Valenzuela, C Fernando et al. "Focus on: neurotransmitter systems." *Alcohol research & health: the journal of the National Institute on Alcohol Abuse and Alcoholism* vol. 34,1 (2011): 106-20.
13. Druse, Mary, et al. "Signaling pathways involved with serotonin1A agonist-mediated neuroprotection against ethanol-induced apoptosis of fetal rhombencephalic neurons." *Developmental Brain Research* 159.1 (2005): 18-28. Print.
14. Lovinger, David M. "Serotonin's Role in Alcohol's Effects on the Brain." *Neurotransmitter Review* 21 (1997): 114-20. Print.
15. Rosling, Claire. "Serotonin: A Molecule of Happiness." *University of Bristol*, http://www.chm.bris.ac.uk/motm/serotonin/depression.htm.
16. National Center for Biotechnology Information. *PubChem Database*. Serotonin, CID=5202, https://pubchem.ncbi.nlm.nih.gov/compound/Serotonin (accessed on Jan. 7, 2020).
17. "Serotonin Synthesis and Metabolism." *Sigma*, https://www.sigmaaldrich.com/technical-documents/articles/biology/rbi-

handbook/non-peptide-receptors-synthesis-and-metabolism/serotonin-synthesis-and-metabolism.html.

18. "The Role of Serotonin in the Central Nervous System." *Canadian Medical Association journal* 75.9 (1956): 765-66. Print.

19. Bertrand, Paul P., and Rebecca L. Bertrand. "Serotonin release and uptake in the gastrointestinal tract." *Autonomic neuroscience: basic & clinical* 153.1-2 (2010): 47-57. Print.

20. Frishman, William H., and Pam Grewall. "Serotonin and the heart." *Annals of Medicine* 32.3 (2000): 195-209. Print.

21. Libretexts. "Hydrogen Bonding." *Chemistry LibreTexts*, Libretexts, 30 Sept. 2019. Web.

22. National Center for Biotechnology Information. PubChem Database. Ethanol, CID=702, https://pubchem.ncbi.nlm.nih.gov/compound/Ethanol (accessed on Jan. 7, 2020)

23. National Center for Biotechnology Information. PubChem Database. Methanol, CID=887, https://pubchem.ncbi.nlm.nih.gov/compound/Methanol (accessed on Jan. 7, 2020)

24. Bursey, Maurice M. "A Brief History of Spectroscopy." *Access Science*, McGraw-Hill Education, Jan. 2017.

25. Robinson, J.W., E.M.S. Frame, and G.M.F. II, "Undergraduate Instrumental Analysis." 7 ed. 2014: CRC Press. Print.

26. Engel, T. and P. Reid, "Physical Chemistry." 3 ed. 2013: Pearson. Print.

27. Larkin, Peter. "Chapter 1 - Introduction: Infrared and Raman Spectroscopy." *Infrared and Raman Spectroscopy*. Ed. Larkin, Peter. Oxford: Elsevier, 2011. 1-5. Print.

28. Christian, Gary D., Purnendu, Dasgupta K., Schug, Kevin A. *Analytical Chemistry*. Ed. Recter, Petra. 7 ed. Danvers, MA: John Wiley & Sons, Inc., 2014. Print.

29. Baena, Josefa Rodríguez and Bernhard Lendl. "Raman spectroscopy in chemical bioanalysis." *Current opinion in chemical biology* 8 5 (2004): 534-9 .

30. Tzontonel. "Quantum and Classical Raman Theory." *Romanian Database of Raman Spectroscopy*, 14 Aug. 2017, http://www.rdrs.ro/blog/quantum-classical-raman-theory/.

31. Gardiner, Derek J. *Practical Raman Spectroscopy*. Ed. Springer-Verlag. Berlin, Germany1989. Print.

32. Fowles, Grant R.; Cassiday, George L. (1986), *Analytic Mechanics* (5th ed.), Fort Worth: Saunders College Publishing, ISBN 0-03-96746-5. Print.

33. McHale, Jeanne L. Molecular Spectroscopy. Boca Raton: CRC, 2017. Print.

34. Bayari, Sevgi, Semran Saglam, and Hasan Ustundag. "Experimental and theoretical studies of the vibrational spectrum of 5-hydroxytryptamine." *Journal of Molecular Structure: THEOCHEM* 726 (2005): 225-32. Print.

35. LeGreve, Tracy A., William H. James Iii, and Timothy S. Zwier. "Solvent Effects on the Conformational Preferences of Serotonin: Serotonin−(H2O)n, n = 1,2." *The Journal of Physical Chemistry A* 113.2 (2009): 399-410. Print.

36. Priya, Mano, L. Senthilkumar, and P. Kolandaivel. "Hydrogen-bonded complexes of serotonin with methanol and ethanol: A DFT study." *Structural Chemistry* 25 (2014). Print.

37. Jha, Omkant, and R. A. Yadav. "Structural and vibrational investigations of a neurotransmitter molecule: Serotonin (5-hydroxy tryptamine)." *Journal of Molecular Structure* 1123 (2016): 92-110. Print

38. Manciu, S. Felicia, et al. "Analysis of Serotonin Molecules on Silver Nanocolloids—A Raman Computational and Experimental Study." *Sensors* 17.7 (2017). Print.

39. Song, Ping, et al. "SERS and in situ SERS spectroelectrochemical investigations of serotonin monolayers at a silver electrode." *Journal of Electroanalytical Chemistry* 688 (2013): 384-91. Print.

40. Qiu, C., et al. "Ultrasensitive detection of neurotransmitters by surface enhanced raman spectroscopy for biosensing applications." *Biointerface Research in Applied Chemistry* 7.1 (2017): 1921-26. Print.

41. Manciu, Felicia S., et al. "Simultaneous Detection of Dopamine and Serotonin-A Comparative Experimental and Theoretical Study of Neurotransmitter Interactions." *Biosensors* 9.1 (2018): 3. Print.

42. Borah, Mukunda Madhab, and Th Gomti Devi. "Vibrational study and Natural Bond Orbital analysis of serotonin in monomer and dimer states by density functional theory." *Journal of Molecular Structure* 1161 (2018): 464-76. Print.

43. McDouall, Joseph J W. "Computational Quantum Chemistry." *Google Books*, RSC Publishing, 2013, https://books.google.com/books.

44. Hehre, Warren J. *A Guide to Molecular Mechanics and Quantum Chemical Calculations*. Wavefunction, 2003.

45. "Crystal Structure." *ScienceDaily: Reference Terms*, ScienceDaily, www.sciencedaily.com/terms/crystal_structure.htm.

46. Cuellar, Kristina A. *Noncovalent Interactions Involving Microsolvated Networks of Trimethylamine-N-Oxide*. University of Mississippi, 2014.

References for Adapted Image Figures

Figure 1.1.1.1: Atomic Structure Labeled, Adapted From (AF) [1]

Figure 1.1.1.2: Intramolecular and Intermolecular bonding

- (AF): https://www.khanacademy.org/test-prep/mcat/chemical-processes/covalent-bonds/

Figure 1.1.2.1: Hydrogen Bonding General Structure

- (AF): https://www.studyorgo.com/blog/how-do-you-to-tell-when-a-hydrogen-bond-will-occur

Figure 1.2.2.1: Neurotransmitter Release and Structure of the Synaptic Cleft, (AF) [8]

Figure 1.2.3.1.1: Life Cycle of a Neurotransmitter, (AF) [9]

Figure 1.3.2.1: Series of reactions deriving Serotonin from L-tryptophan

- (AF): https://www.researchgate.net/publication/273640973_Serotonin_serotonin_receptors

Figure 1.5.1.1: The Electromagnetic Spectrum, (AF) [26]

Figure 1.5.2.1: Energy level diagram describing allowed transitions, (AF) [26]

Figure 1.5.4.1: Vibrational modes as differentiated by motion

- (AF): https://www.semanticscholar.org/paper/IR-spectroscopy-for-vibrational-modes

Figure 1.6.2.1: Diagram of Rayleigh and Raman (stokes / anti-stokes) processes

- (AF):https://www.researchgate.net/publication/275274523_Evaluating_Lignocellulosic_Biomass

Figure 1.7.1: ΔE of ethane as a function of the $<_{torsion}$ about the C-C bond, (AF) [43]

Figure 2.1: FTIR Spectrum of 5-HT in KBr, [34]

Figure 2.2: LE conformers of a serotonin-water cluster, [35]

Figure 2.3: RDIR spectra of Serotonin-water clusters compared with theory, [35]

Figure 2.4: Experimental Raman Spectrum of Serotonin, [37]

Figure 2.5: Experimentally measured / calculated Raman vibrations of Serotonin, [38]

Figure 2.6: SERS theoretical / experimental analysis for three serotonin conformers, [38]

Figure 2.7: Simulated and Experimental spectra of Serotonin, [42]

Figure 4.1: Horiba LabRAM Confocal Spectrometer

- https://www.horiba.com/en_en/products/detail/action/show/Product/labram-hr-evolution-1083/